US008068216B2

(12) **United States Patent**
Caldwell et al.

(10) **Patent No.: US 8,068,216 B2**
(45) **Date of Patent: *Nov. 29, 2011**

(54) **OPTICAL AIR DATA SYSTEMS AND METHODS**

(75) Inventors: **Loren M. Caldwell**, Fort Collins, CO (US); **Shoou-Yu Tang**, Fort Collins, CO (US); **Martin J. O'Brien**, Conifer, CO (US)

(73) Assignee: **Ophir Corporation**, Littleton, CO (US)

(*) Notice: Subject to any disclaimer, the term of this patent is extended or adjusted under 35 U.S.C. 154(b) by 288 days.

This patent is subject to a terminal disclaimer.

(21) Appl. No.: **12/268,072**

(22) Filed: **Nov. 10, 2008**

(65) **Prior Publication Data**

US 2010/0277715 A1 Nov. 4, 2010

Related U.S. Application Data

(60) Division of application No. 11/488,259, filed on Jul. 17, 2006, now Pat. No. 7,564,539, and a continuation-in-part of application No. 11/103,020, filed on Apr. 11, 2005, now Pat. No. 7,400,385, which is a continuation of application No. 10/632,735, filed on Aug. 1, 2003, now Pat. No. 6,894,768.

(60) Provisional application No. 60/699,630, filed on Jul. 15, 2005, provisional application No. 60/400,462, filed on Aug. 2, 2002.

(51) **Int. Cl.**
G01P 3/36 (2006.01)
G01N 21/00 (2006.01)

(52) **U.S. Cl.** **356/28.5**; 356/337

(58) **Field of Classification Search** 356/28, 356/28.5, 337, 342

See application file for complete search history.

(56) **References Cited**

U.S. PATENT DOCUMENTS

4,483,614	A	11/1984	Rogers
4,988,190	A	1/1991	Miles
5,111,055	A	5/1992	Fima
5,267,010	A	11/1993	Kremer et al.
5,285,256	A	2/1994	Nelson et al.
5,394,238	A	2/1995	Mocker et al.

(Continued)

FOREIGN PATENT DOCUMENTS

EP 1158300 11/2001

(Continued)

OTHER PUBLICATIONS

Grinstead, J.H., et al "Frequency-Modulated Filtered Rayleigh Scattering (FM-FRS): A New Technique for Real-Time Velocimetry" paper 96-0302, American Institute of Aeronautics and Astronautics, Inc., pp. 1-11, 1996.

(Continued)

Primary Examiner — Isam Alsomiri

(74) *Attorney, Agent, or Firm* — Lathrop & Gage LLP

(57) **ABSTRACT**

A method for remotely sensing air outside a moving aircraft includes generating laser radiation within a swept frequency range. A portion of the laser radiation is projected from the aircraft into the air to induce scattered laser radiation. Filtered scattered laser radiation, filtered laser radiation, and unfiltered laser radiation are detected. At least one actual ratio is determined from data corresponding to the filtered scattered laser radiation and the unfiltered laser radiation. One or more air parameters are determined by correlating the actual ratio to at least one reference ratio.

6 Claims, 9 Drawing Sheets

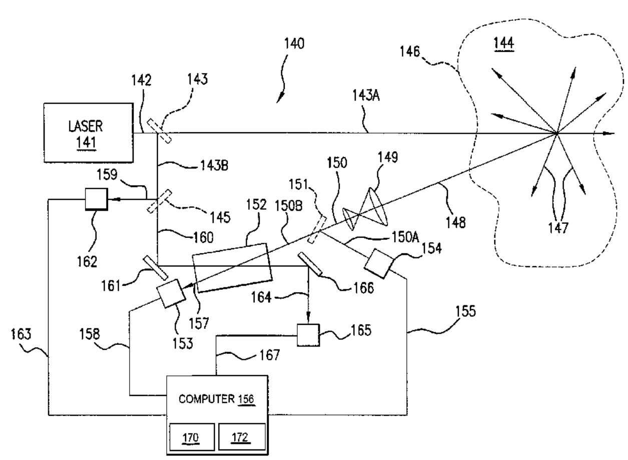

U.S. PATENT DOCUMENTS

5,835,252 A	11/1998	Meier et al.	
6,307,626 B1	10/2001	Miles et al.	
6,512,996 B1	1/2003	Praskovsky et al.	
7,106,447 B2	9/2006	Hays	
7,400,385 B2 *	7/2008	Caldwell et al.	356/28
7,580,127 B1	8/2009	Mayor et al.	
2004/0027570 A1	2/2004	Caldwell et al.	
2004/0263826 A1	12/2004	Langdon	
2006/0140764 A1	6/2006	Smith et al.	
2007/0109528 A1	5/2007	Caldwell et al.	
2009/0046289 A1	2/2009	Caldwell et al.	
2009/0051896 A1	2/2009	Caldwell et al.	

FOREIGN PATENT DOCUMENTS

WO	WO9935519	7/1999
WO	WO2004077067	9/2004

OTHER PUBLICATIONS

Ed.Boutier, A New Trends in Instrumentation for Hypersonic Research, Seasholtz, R. G. 1993: “2D Velocity and Temperature Measurements in High Speed Flows Based on Spectrally Resolved Rayleigh Scattering”, Advanced Research NATO Workshop, ONERA, Le Fauga-Muazac, France, Apr. 27-May 1, 399-408.

Kliner, D. A. V., et al,; 2002: “Efficient Second, Third, Fourth, and Fifth Harmonic Generation of Yb-Doped Fiber Amplifier”, Optics Communications, 210, 393-398.

Korb, C.L.; Gentry, B. M.; Weng, C.Y. 1992: “Edge Technique: Theory and Application to the Lidar Measurement of Atmospheric Wind,” Applied Optics, 31, 4202.

Miles, R. B.; et al., 1992: “Filtered Rayleigh Scattering Measurements in Supersonic/Hypersonic Facilities”, AIAA 17th Aerospace Ground Testing Conference, paper AIAA-92-3894, pp. 1-10.

Philippe, L. C. & Hanson, R.K. 1993: “Laser Diode Wavelength-Modulation Spectroscopy for Simultaneous Measurement of Temperature, Pressure, and Velocity in Shock-Heated Oxygen Flows”, Applied Optics, 32, 6090-6103.

She, C. Y.,et al.; 1992: “High Spectral-Resolution Rayleigh-Mie Lidar Measurment of Aerosol and Atmospheric Profiles”, Optics Letters, 17, 541.

Shimizu, H. et al., “High spectral resolution lidar system with atomic blocking filters for measuring atmospher parameters,” Applied Optics 22, 1372-1381 (1983).

Wu, Y., et al.; 1995: “New Method for Acquiring a High-Resolution Atomospheric Rayleigh-Mie Spectrum”, Optical Engineering, Apr., 34, No. 4, 1195-1199.

Yalin, A.P. & Miles, R. B. 1999: “Ultraviolet Filtered Rayleigh Scattering Temperature Measurements with a Mercury Filter”, Optics Letters, 24, 590-592.

Tenti, G., et al., 1974: “On the Kinetic Model Description of Rayleigh-Brillouin Scattering From Molecular Glasses”, Canadian Journal of Physics, 52, 285-290.

Alvarez II, R. J., et al., 1993: “Profiling Temperature, Pressure, and Aerosol Properties Using a High Spectral Resolution Lidar Employing Atomic Blocking Filters”, Journal of Atmospheric and Oceanic Technology, 10, 546.

PCT Application No. PCT/US03/24191; International Search Report dated Mar. 17, 2004, 7 pages.

U.S. Appl. No. 10/632,735.

U.S. Appl. No. 11/103,020.

U.S. Appl. No. 11/488,259; Restriction Requirement mailed Jun. 27, 2008; 7 pages.

U.S. Appl. No. 11/488,259; Response to Restriction Requirement; filed Jul. 28, 2008; 5 pages.

U.S. Appl. No. 11/488,259; Office Action mailed Nov. 14, 2008; 8 pages.

U.S. Appl. No. 11/488,259; Response to Office Action filed Feb. 16, 2009; 11 pages.

Canadian Application 2,494,458, Office Action dated Feb. 5, 2008.

Canadian Application 2,494,458, Response to Office Action filed Aug. 5, 2008.

European Application EP 03 749 002.6, Letter and formal drawings; Feb. 11, 2005; 12 pages.

European Application EP 03 749 002.6, Amendment; Mar. 10, 2005, 14 pages.

European Application EP 03 749 002.6, Amendment; Apr. 13, 2005; 9 pages.

European Application EP 03 749 002.6, Examination Report dated Mar. 2, 2006; 6 pages.

European Application EP 03 749 002.6, Reply to Examination Report filed Aug. 25, 2006; 36 pages.

European Application EP 03 749 002.6, Invitation Pursuant to Article 96(2) and Rule 51(2); Consultation by Telephone; Nov. 17, 2006; 3 pages.

European Application EP 03 749 002.6, Result of Consultation by Telephone and Form 2036; Nov. 24, 2006; 2 pages.

European Application EP 03 749 002.6, Communication about intention to grant a European patent; Dec. 8, 2006; 6 pages.

European Application EP 03 749 002.6, Letter dated Mar. 15, 2007; 1 page.

European Application EP 03 749 002.6, Decision to Grant a European Patent, Apr. 5, 2007; 2 pages.

U.S. Appl. No. 12/140,186, Notice of Allowance mailed Mar. 9, 2010, 6 pages.

U.S. Appl. No. 12/140,186, Examiner Interview Summary mailed Jan. 22, 2010, 3 pages.

U.S. Appl. No. 12/140,186, Response to Interview Summary and Notice of Incomplete Reply filed Jan. 22, 2010, 11 pages.

European Application No. 09160572.5 Search Report, Sep. 25, 2009, 5 pages.

U.S. Appl. No. 11/488,259 Notice of Allowance mailed Apr. 16, 2009, 4 pages.

U.S. Appl. No. 11/488,259 Issue Fee Payment, Jun. 16, 2009, 1 page.

Canadian Application 2,494,458 Notice of Allowance dated Feb. 20, 2009, 1 page.

U.S. Appl. No. 12/140,186 Office Action mailed Jul. 22, 2009, 8 pages.

U.S. Appl. No. 12/140,186 Response to Office Action filed Oct. 22, 2009, 16 pages.

U.S. Appl. No. 12/268,277 Notice of Allowance mailed Oct. 8, 2010, 7 pages.

* cited by examiner

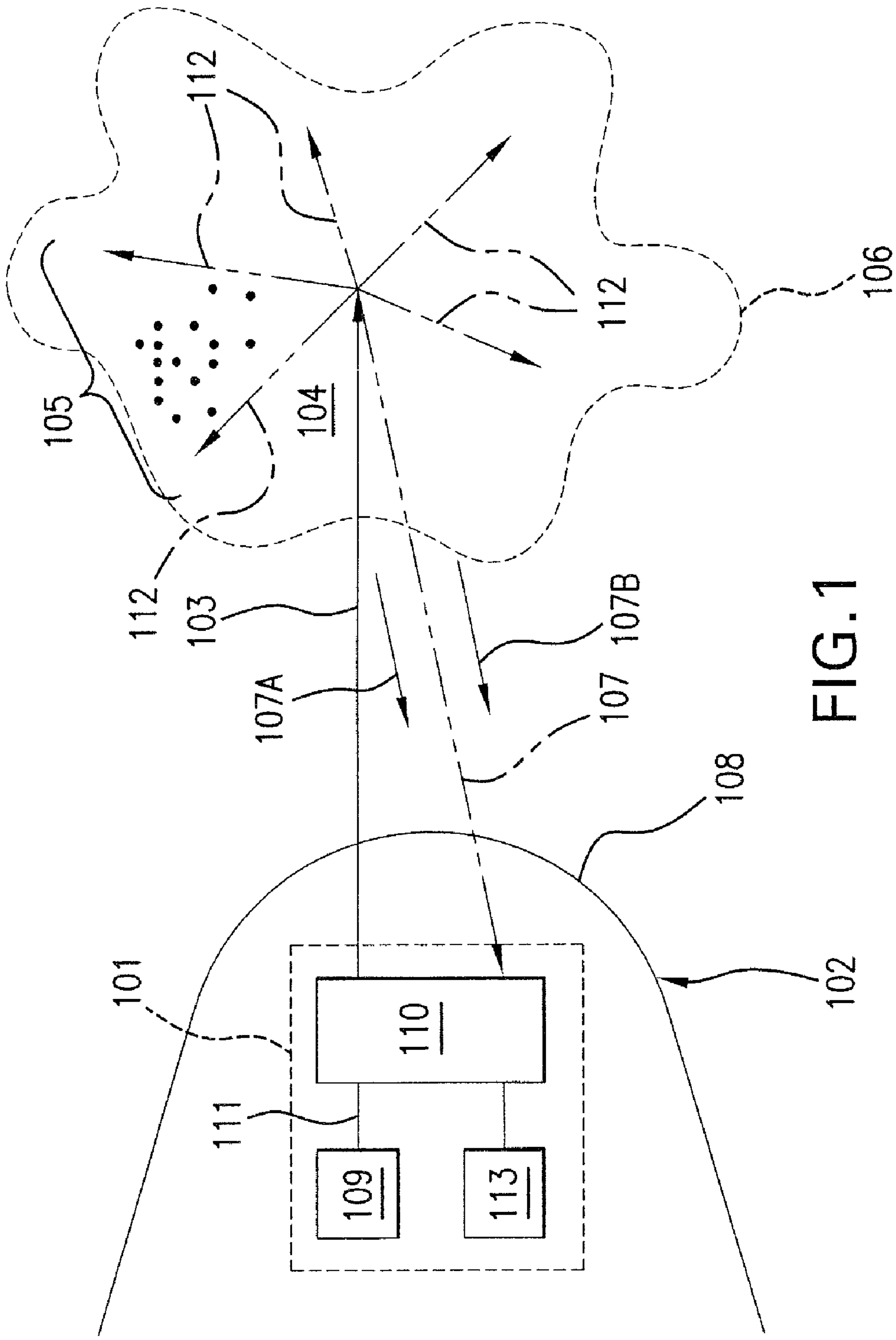
112
112
106
105
104
112
103
107A
107B
107
108
101
110
111
109
113
102

FIG. 1

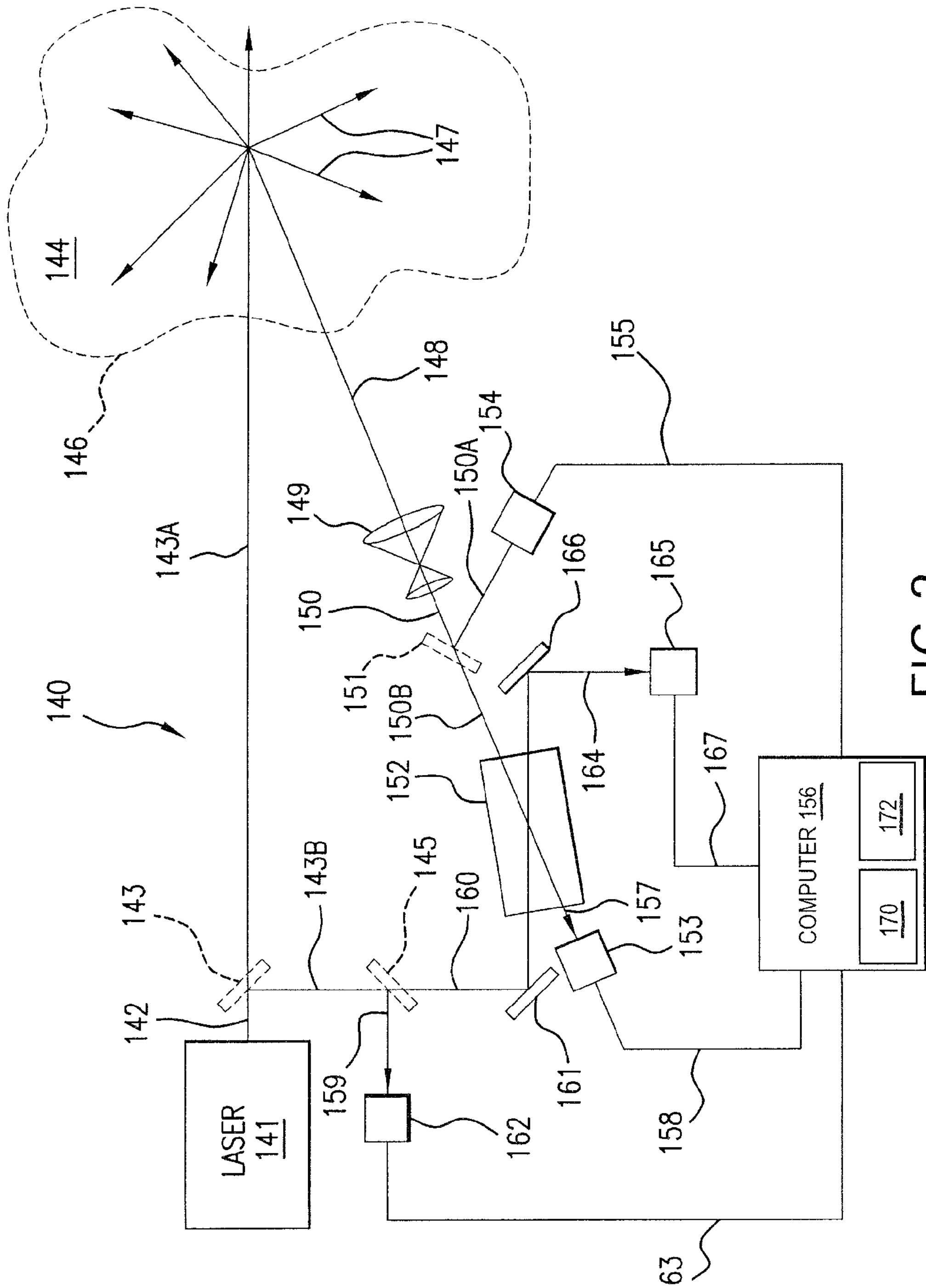
140
141
LASER
142
143
143A
143B
144
145
146
147
148
149
150
150A
150B
151
152
153
154
155
COMPUTER 156
157
158
159
160
161
162
163
164
165
166
167
170
172

FIG. 2

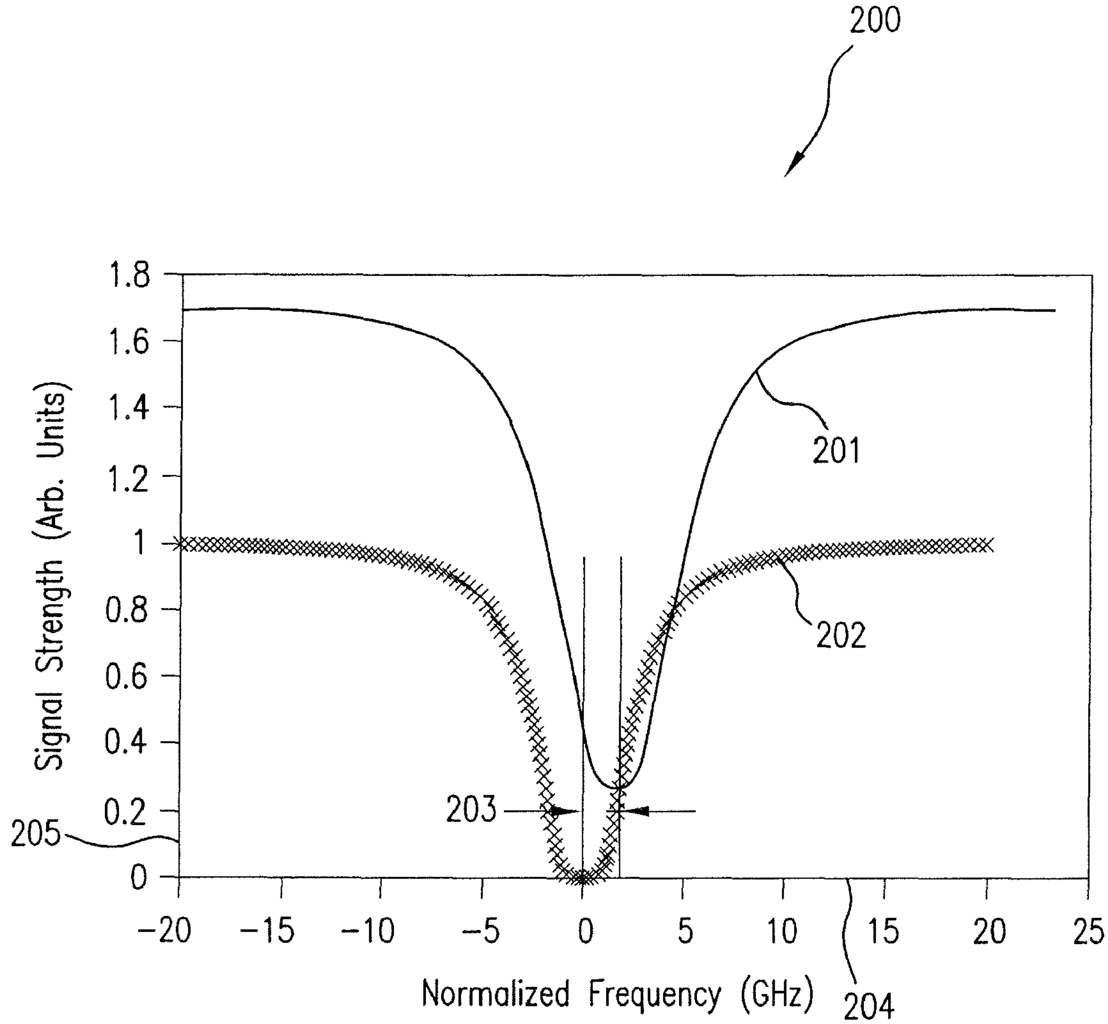
200
1.8
1.6
1.4
1.2
1
0.8
0.6
0.4
0.2
0
Signal Strength (Arb. Units)
201
202
203
205
204
−20
−15
−10
−5
0
5
10
15
20
25
Normalized Frequency (GHz)

FIG.3

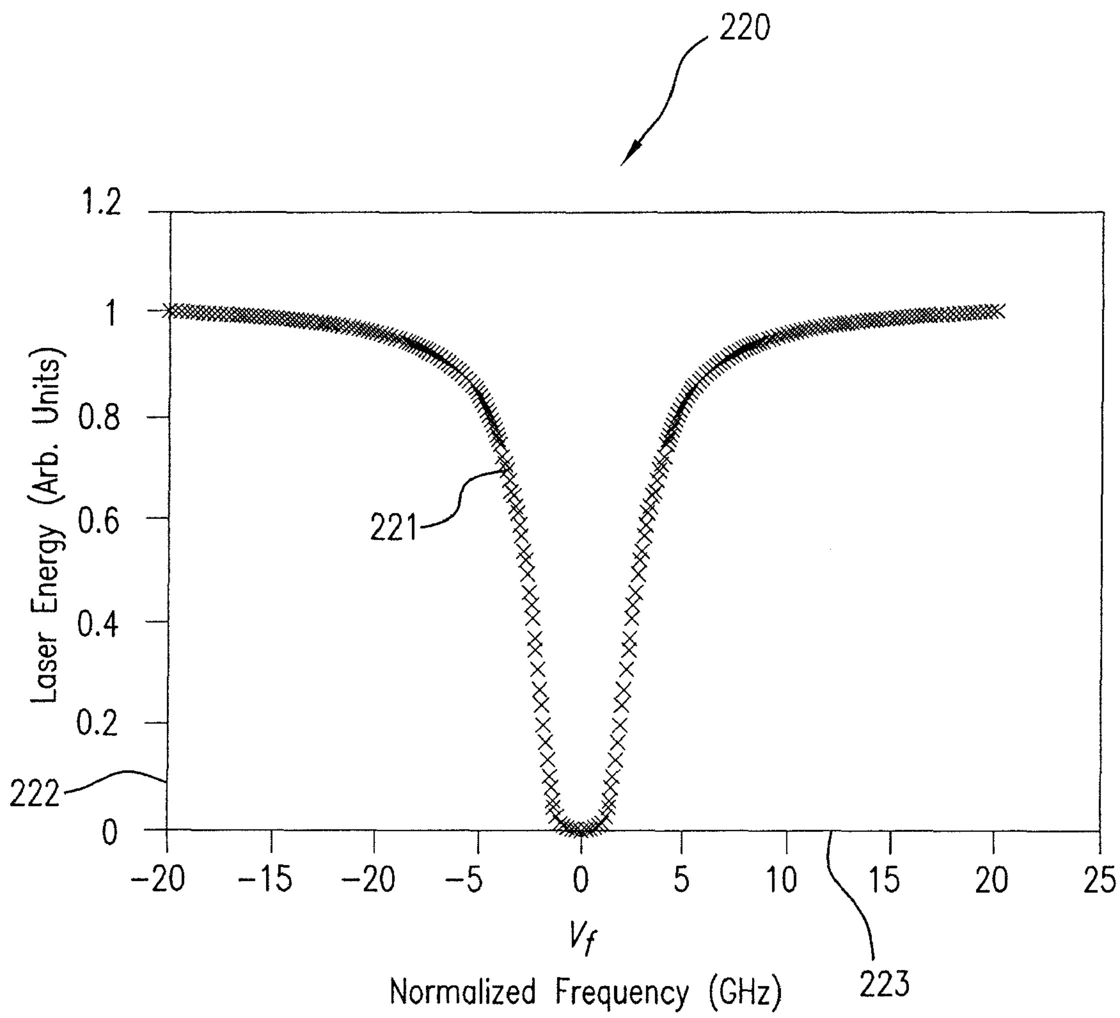
220
1.2
1
0.8
0.6
0.4
0.2
0
Laser Energy (Arb. Units)
221
222
−20 −15 −20 −5 0 5 10 15 20 25
V_f
Normalized Frequency (GHz)
223

FIG.4

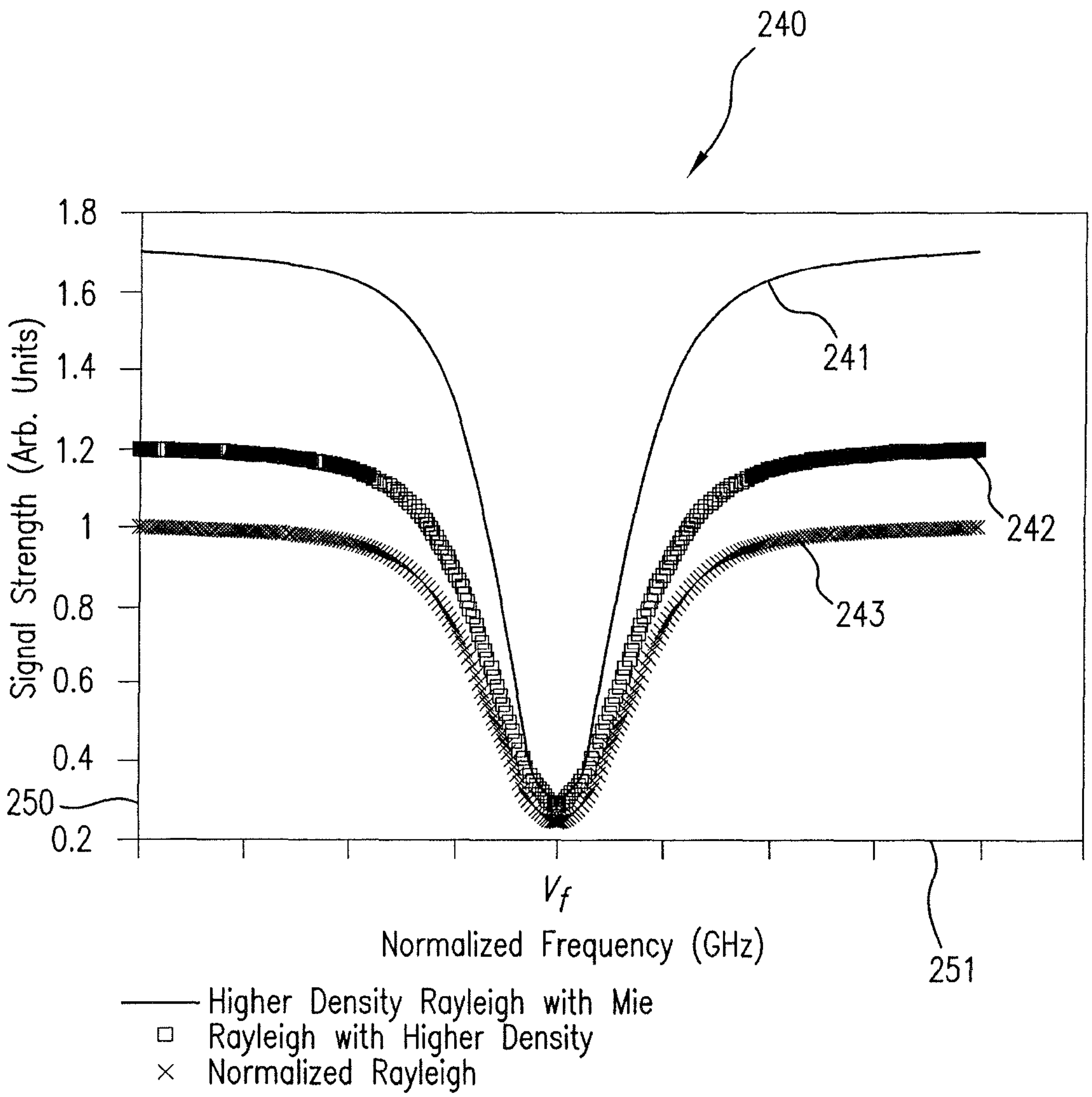
240
1.8
1.6
1.4
1.2
1
0.8
0.6
0.4
250
0.2
Signal Strength (Arb. Units)
241
242
243
V_f
Normalized Frequency (GHz)
251
Higher Density Rayleigh with Mie
Rayleigh with Higher Density
Normalized Rayleigh

FIG.5

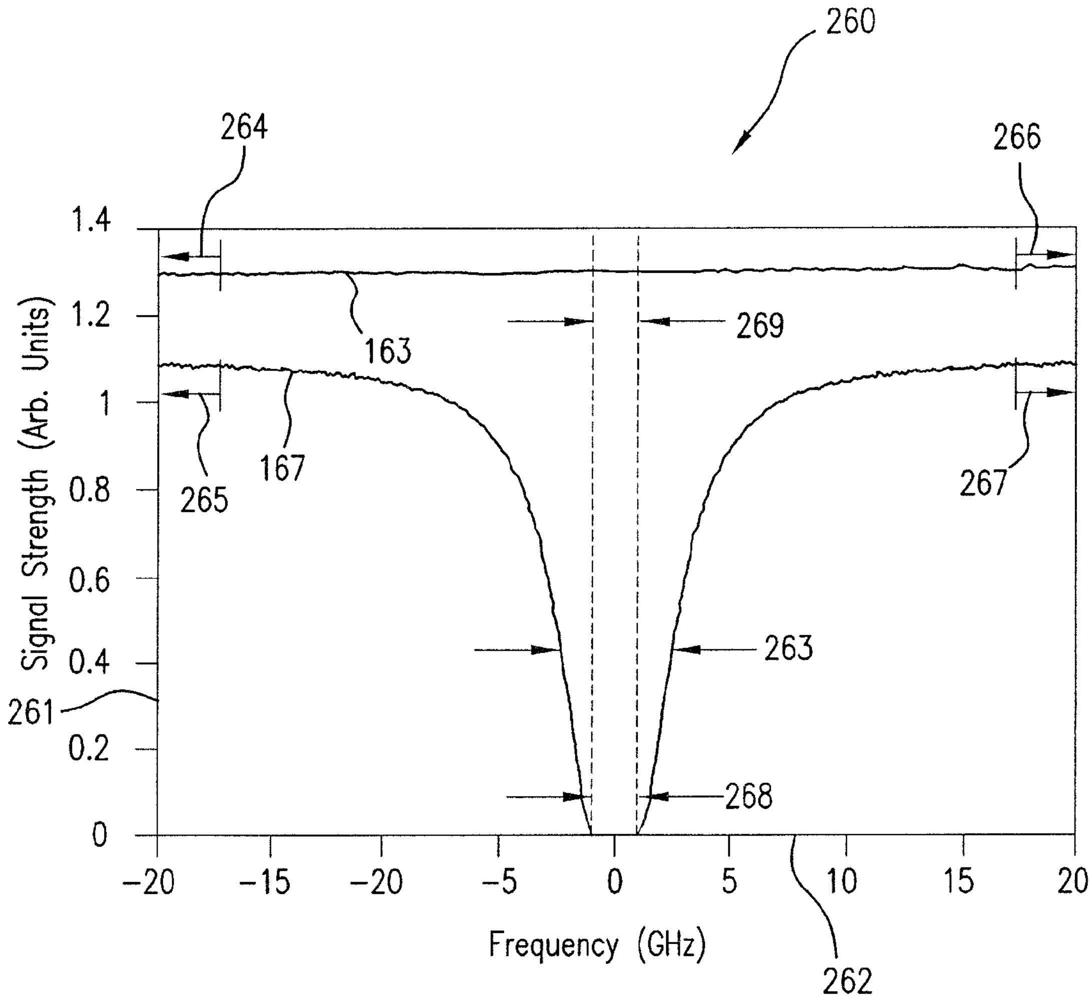
260
264
266
1.4
1.2
1
0.8
0.6
0.4
0.2
0
Signal Strength (Arb. Units)
163
269
167
265
267
263
261
268
−20
−15
−20
−5
0
5
10
15
20
Frequency (GHz)
262

FIG.6

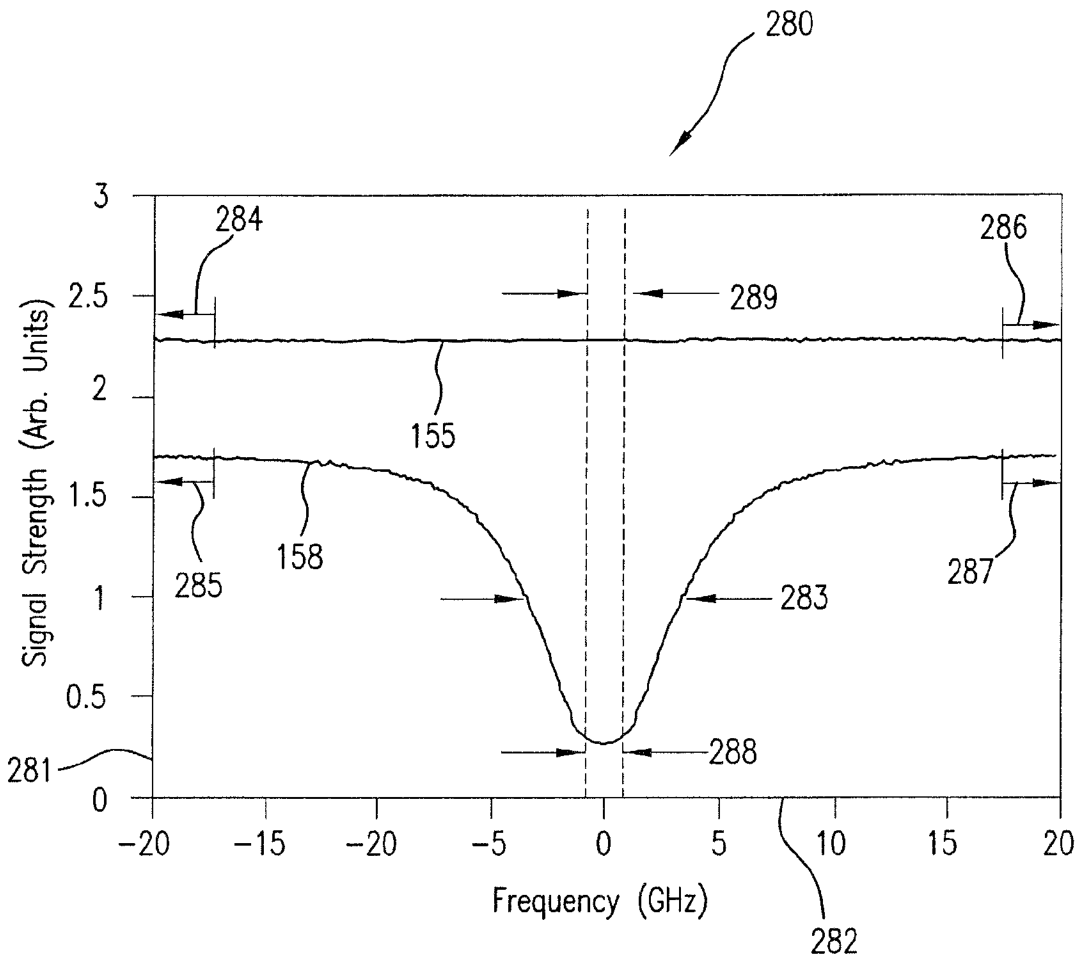

280
3
2.5
2
1.5
1
0.5
0
284
286
289
155
285
158
283
287
281
288
282
−20
−15
−20
−5
0
5
10
15
20
Signal Strength (Arb. Units)
Frequency (GHz)

FIG. 7

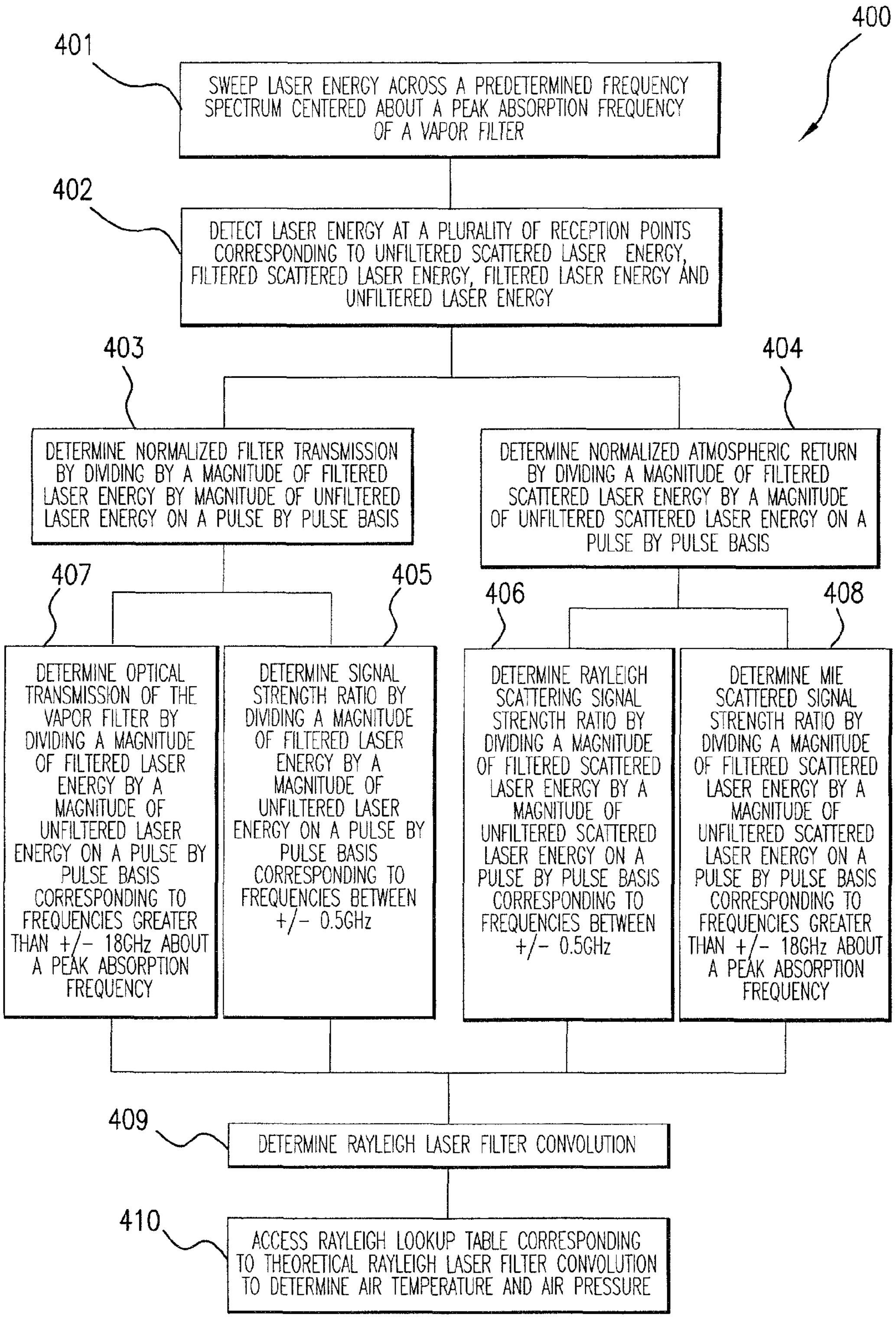
400
401
SWEEP LASER ENERGY ACROSS A PREDETERMINED FREQUENCY SPECTRUM CENTERED ABOUT A PEAK ABSORPTION FREQUENCY OF A VAPOR FILTER
402
DETECT LASER ENERGY AT A PLURALITY OF RECEPTION POINTS CORRESPONDING TO UNFILTERED SCATTERED LASER ENERGY, FILTERED SCATTERED LASER ENERGY, FILTERED LASER ENERGY AND UNFILTERED LASER ENERGY
403
DETERMINE NORMALIZED FILTER TRANSMISSION BY DIVIDING BY A MAGNITUDE OF FILTERED LASER ENERGY BY MAGNITUDE OF UNFILTERED LASER ENERGY ON A PULSE BY PULSE BASIS
404
DETERMINE NORMALIZED ATMOSPHERIC RETURN BY DIVIDING A MAGNITUDE OF FILTERED SCATTERED LASER ENERGY BY A MAGNITUDE OF UNFILTERED SCATTERED LASER ENERGY ON A PULSE BY PULSE BASIS
407
DETERMINE OPTICAL TRANSMISSION OF THE VAPOR FILTER BY DIVIDING A MAGNITUDE OF FILTERED LASER ENERGY BY A MAGNITUDE OF UNFILTERED LASER ENERGY ON A PULSE BY PULSE BASIS CORRESPONDING TO FREQUENCIES GREATER THAN +/- 18GHz ABOUT A PEAK ABSORPTION FREQUENCY
405
DETERMINE SIGNAL STRENGTH RATIO BY DIVIDING A MAGNITUDE OF FILTERED LASER ENERGY BY A MAGNITUDE OF UNFILTERED LASER ENERGY ON A PULSE BY PULSE BASIS CORRESPONDING TO FREQUENCIES BETWEEN +/- 0.5GHz
406
DETERMINE RAYLEIGH SCATTERING SIGNAL STRENGTH RATIO BY DIVIDING A MAGNITUDE OF FILTERED SCATTERED LASER ENERGY BY A MAGNITUDE OF UNFILTERED SCATTERED LASER ENERGY ON A PULSE BY PULSE BASIS CORRESPONDING TO FREQUENCIES BETWEEN +/- 0.5GHz
408
DETERMINE MIE SCATTERED SIGNAL STRENGTH RATIO BY DIVIDING A MAGNITUDE OF FILTERED SCATTERED LASER ENERGY BY A MAGNITUDE OF UNFILTERED SCATTERED LASER ENERGY ON A PULSE BY PULSE BASIS CORRESPONDING TO FREQUENCIES GREATER THAN +/- 18GHz ABOUT A PEAK ABSORPTION FREQUENCY
409
DETERMINE RAYLEIGH LASER FILTER CONVOLUTION
410
ACCESS RAYLEIGH LOOKUP TABLE CORRESPONDING TO THEORETICAL RAYLEIGH LASER FILTER CONVOLUTION TO DETERMINE AIR TEMPERATURE AND AIR PRESSURE

FIG. 8

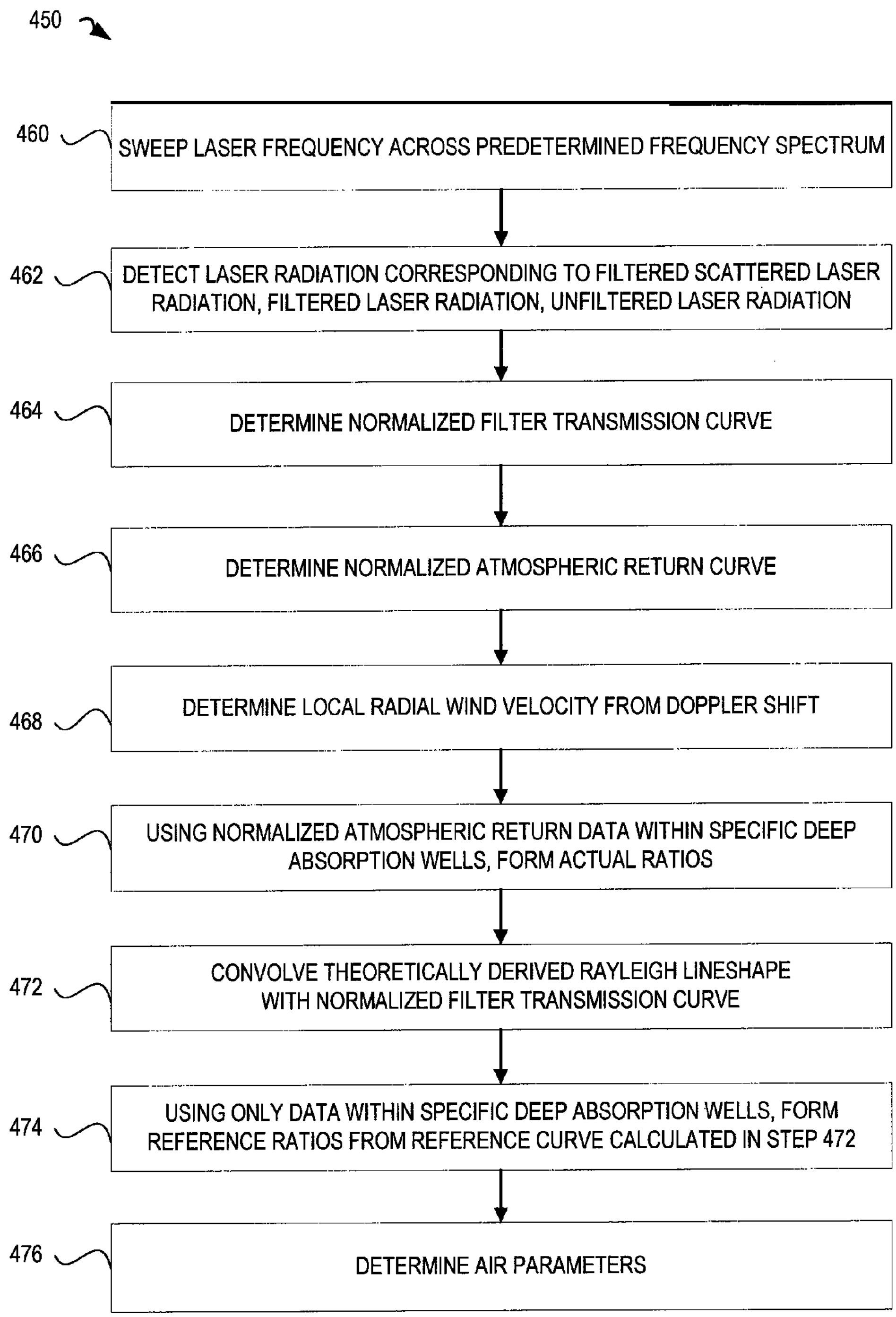
450
460
SWEEP LASER FREQUENCY ACROSS PREDETERMINED FREQUENCY SPECTRUM
462
DETECT LASER RADIATION CORRESPONDING TO FILTERED SCATTERED LASER RADIATION, FILTERED LASER RADIATION, UNFILTERED LASER RADIATION
464
DETERMINE NORMALIZED FILTER TRANSMISSION CURVE
466
DETERMINE NORMALIZED ATMOSPHERIC RETURN CURVE
468
DETERMINE LOCAL RADIAL WIND VELOCITY FROM DOPPLER SHIFT
470
USING NORMALIZED ATMOSPHERIC RETURN DATA WITHIN SPECIFIC DEEP ABSORPTION WELLS, FORM ACTUAL RATIOS
472
CONVOLVE THEORETICALLY DERIVED RAYLEIGH LINESHAPE WITH NORMALIZED FILTER TRANSMISSION CURVE
474
USING ONLY DATA WITHIN SPECIFIC DEEP ABSORPTION WELLS, FORM REFERENCE RATIOS FROM REFERENCE CURVE CALCULATED IN STEP 472
476
DETERMINE AIR PARAMETERS

FIG. 9

OPTICAL AIR DATA SYSTEMS AND METHODS

CROSS-REFERENCE TO RELATED APPLICATIONS

This application is a divisional of U.S. patent application Ser. No. 11/488,259 filed 17 Jul. 2006 now U.S. Pat. No. 7,564,539, which claims benefit of priority to U.S. Provisional Patent Application Ser. No. 60/699,630 filed Jul. 15, 2005. U.S. patent application Ser. No. 11/488,259 is also a continuation-in-part of U.S. patent application Ser. No. 11/103,020 filed 11 Apr. 2005, now U.S. Pat. No. 7,400,385, which is a continuation of U.S. patent application Ser. No. 10/632,735 filed Aug. 1, 2003, now U.S. Pat. No. 6,894,768, which claims benefit of priority to U.S. Provisional Patent Application Ser. No. 60/400,462 filed Aug. 2, 2002. All of the aforementioned applications are hereby incorporated herein by reference.

U.S. GOVERNMENT RIGHTS

This invention was made in part with the support of the U.S. Government; the U.S. Government has certain rights in this invention as provided for by the tennis of Grant #NAS4-02043 awarded by the NASA Dryden Flight Research Center.

BACKGROUND

An Air Data System ("ADS") provides sensed telemetry informing pilots, navigators or Vehicle Management System computers of air parameter(s) affecting aircraft stability. These air parameters include, for example, air speed, air temperature and air pressure, each being useful for navigation and flight control. The ADS exists in many forms, for example, as mechanical, opto-mechanical or opto-electronic devices.

An Optical Air Data System ("OADS") uses light to determine parameters of air speed. The OADS transmits light pulses into the atmosphere and receives light that aerosols reflect or "backscatter" towards the aircraft. Aerosols are fine solids and/or liquid particles suspended in air or other gases. The OADS may also measure the Doppler effect by receiving backscattered light and measuring its return frequency to determine speed. Certain prior art OADSs rely on scattered light that is unpredictable because of aerosol distributions that vary significantly with altitude and cloud content. In addition, some regions of the atmosphere contain too few aerosols to enable reliable air data measurements, and such an OADS cannot determine air temperature or air pressure.

SUMMARY

In an embodiment, a method for remotely sensing air outside a moving aircraft includes generating laser radiation within a swept frequency range. A portion of the laser radiation is projected from the aircraft into the air to induce scattered laser radiation. Filtered scattered laser radiation, filtered laser radiation, and unfiltered laser radiation are detected. At least one actual ratio is determined from data corresponding to the filtered scattered laser radiation and the unfiltered laser radiation. One or more air parameters are determined by correlating the actual ratio to at least one reference ratio.

In an embodiment, a method for remotely sensing air outside a moving aircraft includes generating laser radiation within a swept frequency range, wherein the swept frequency range includes at least two absorption features of at least one band stop filter. A portion of the laser radiation is projected from the aircraft into the air to induce scattered radiation Filtered scattered laser radiation, filtered laser radiation, and unfiltered laser radiation are detected. A normalized atmospheric return curve is determined from the filtered scattered laser radiation and the unfiltered laser radiation; a normalized filter transmission curve is determined from the filtered laser radiation and the unfiltered laser radiation. At least one actual ratio is determined from the normalized atmospheric return curve. At least one reference ratio is determined from the normalized filter transmission curve and a Rayleigh line shape corresponding to one or more estimated air parameters. One or more air parameters are determined by correlating the at least one actual ratio to the at least one reference ratio.

In an embodiment, a method for remotely sensing air outside a moving aircraft includes generating laser radiation within a swept frequency range. A portion of the laser radiation is projected from the aircraft into the air to induce scattered radiation. Filtered scattered laser radiation, filtered laser radiation, unfiltered scattered laser radiation, and unfiltered laser radiation are detected. A normalized filter transmission and a normalized atmospheric return are determined from the filtered scattered laser radiation, filtered laser radiation, unfiltered scattered laser radiation, and unfiltered laser radiation. A plurality Doppler line shifts and a plurality of radial wind velocities are determined from a plurality of frequency shifts between the normalized filter transmission and the normalized atmospheric return, wherein each frequency shift corresponds to an absorption feature of at least one band stop filter.

In an embodiment, a system for sensing of air outside a moving aircraft includes at least one laser for generating laser radiation and at least one transceiver for projecting the laser radiation to the air and for receiving scattered laser radiation from the air. Additionally, the system includes at least one band stop filter selected from the group consisting of a fixed frequency atomic vapor filter, an interference filter, a dichroic filter, a fiber Bragg grating filter, a Rugate filter, and combinations thereof. Furthermore, the system includes a computer for controlling the laser and for processing signals from the transceiver to determine one or more air parameters based on the scattered laser radiation.

In an embodiment, a software product includes instructions, stored on computer-readable media, wherein the instructions, when executed by a computer, perform steps for remotely sensing air outside a moving aircraft. The software product includes instructions for generating laser radiation within a swept frequency range. The software product also includes instructions for determining a normalized atmospheric return curve from filtered scattered laser radiation and unfiltered laser radiation and instructions for determining a normalized filter transmission curve from filtered laser radiation and the unfiltered laser radiation. Furthermore, the software product includes instructions for determining at least one actual ratio from the normalized atmospheric return curve and instructions for determining at least one reference ratio from the normalized filter transmission curve and a Rayleigh line shape corresponding to one or more estimated air parameters. Also included within the software product are instructions for determining one or more air parameters by correlating the at least one actual ratio to the at least one reference ratio.

BRIEF DESCRIPTION OF THE DRAWINGS

FIG. **1** shows one Optical Air Data System ("OADS"), according to an embodiment.

FIG. **2** shows one OADS, according to an embodiment.

FIG. 3 shows one graph useful in illustrating an exemplary air speed calculation with an OADS, according to an embodiment.

FIGS. 4-7 show graphs illustrating exemplary calculations for other air parameters with an OADS, according to an embodiment.

FIG. 8 is a flowchart showing one exemplary method of operation of an OADS, according to an embodiment.

FIG. 9 is a flowchart showing one exemplary method of operation of an OADS, according to an embodiment.

DETAILED DESCRIPTION OF THE DRAWINGS

FIG. 1 shows one Optical Air Data System ("OADS") **101** mounted on or within an aircraft **102**. In this embodiment, OADS **101** is configured for projecting laser radiation **103** to air **104**. Laser radiation **103** impinges on air **104** and aerosol particles **105** (in air **104**), causing scattering of laser radiation **103**, which is represented in FIG. **1** as a scatter field **106**. Distance between aircraft **102** and scatter field **106** is controlled by overlap between laser radiation **103** and the transceiver **110** field of view at a distance from aircraft **102**, to provide an optimized intensity for return laser radiation **107** and to eliminate possible measurement error arising from displaced air proximate to aircraft **102**. OADS **101** detects backscattered laser radiation **107** that is backscattered from air **104** at laser scatter field **106**. Radiation **107** may be in the ultra-violet (UV) spectrum, for example, having a wavelength within a range of 250 nm to 270 nm; however, other ranges may alternatively be used to produce scatter field **106**.

Return laser radiation **107** typically contains molecular scattered (e.g., Rayleigh) components **107**A and/or aerosol scattered (e.g., Mie) components **107**B. OADS **101** distinguishes the molecular scattered components **107**A from the aerosol scattered components **107**B and correspondingly determines one or more air parameters based on backscattered laser radiation **107**. Examples of such air parameters include air speed, air pressure, air temperature and/or aircraft orientation angles relative to the local wind. OADS **101** may be configured with other aircraft as well, such as unmanned air vehicles (UAVs), helicopters, gliders and space shuttles. Although illustrated within a "nose" **108** of aircraft **102**, OADS **101** may be configured in any other part of aircraft **102**.

As shown in FIG. **1**, OADS **101** includes a laser **109** configured for generating laser radiation **103**. Transceiver **110** is configured for transmitting laser radiation **103**, from laser **109** via optical coupling **111**, and receiving backscattered laser radiation **107**. Optical coupling **111** may exist in the form of a fiber optic connection or free space transmission. Accordingly, transceiver **110** projects the laser radiation as laser radiation **103** to air **104**. Air **104** scatters laser radiation **103** at scatter field **106** in a plurality of directions (e.g., illustrated as vectors **112**). Scatter field **106** also returns, or backscatters, radiation **107** towards transceiver **110**, which subsequently receives the backscattered laser radiation **107**. Transceiver **110** converts backscattered laser radiation **107** to processable electronic signals, via computer **113**, to determine the air parameters.

Computer **113** communicatively couples with transceiver **110** and processes signals from transceiver **110** to distinguish a molecular scattered component **107**A from an aerosol scattered component **107**B. Computer **113** determines the air parameters based on laser radiation **107** backscattered from molecules and/or aerosols in air **104**. Accordingly, as described below, computer **113** may employ one or more digital signal processing algorithms to determine such parameters.

While OADS **101** illustrates one transceiver **110** in an exemplary embodiment, a plurality of transceivers may be used, depending on an application. For example, a helicopter employing OADS **101** may use two transceivers **110** to determine air parameters such as a forward velocity (e.g., air speed) and a horizontal plane, or "yaw", of the helicopter. An airplane may use three transceivers **110** positioned in a particular manner to determine various aircraft geometries, such as angle of attack and sideslip, in addition to the air parameters of air speed, air pressure and air temperature. In addition, air vehicles (fixed wing and rotary) may employ three or more transceivers and/or lasers to increase Optical Air Data System reliability through a redundant system architecture. Using three OADS transceivers mounted orthogonally to one another may fully resolve a total airspeed vector by providing three independent measurements for the air speed vector (i.e., corresponding to three axes of a Cartesian coordinate system). The transceivers are for example located in uncommon planes and their geometry respective of a known aircraft center-line. Vector algebra may then be used to determine the full airspeed vector, including forward air speed, angle-of-sideslip and angle-of-attack.

FIG. 2 shows one OADS **140**. OADS **140** illustrates another embodiment used for determining air parameters, such as those described in FIG. **1**, based upon laser radiation backscattered from both air molecules and aerosols. In this embodiment, OADS **140** includes laser **141** configured for generating laser radiation **142**. Laser **141** may be a tunable laser having a tuned center wavelength of about 253.7 nm, although other wavelengths may be used. For example, laser **141** may be a frequency quadrupled, Nd:YAG (i.e., neodymium:yttrium-aluminum-garnet) pumped Ti:Sapphire (titanium-sapphire) laser. Alternatively, frequency-quadrupled Yb-doped (ytterbium-doped) fiber lasers may be used that offer important benefits of smaller size, lighter weight, increased robustness and improved reliability, as compared to Nd:YAG-pumped Ti:Sapphire lasers. Laser **141** may generate laser radiation that is tunable across a frequency range of about 40 GHz; laser **141** may be a continuous wave laser which sweeps in frequency across this range, or it may be a pulsed laser controlled such that each pulse has a frequency distribution centered about a tunable peak frequency. In one embodiment, the peak frequency increments by about 100 MHz from each pulse to the next. Laser **141** may tune +/−20 GHz about a center frequency of approximately 1182.5 THz, or c/253.7 nm, where c is the speed of light (approximately 3×10^8 m/s). In the illustrated embodiment, laser **141** radiates laser radiation **142** to beam splitter **143**, which splits the beam into two components, **143**A and **143**B. Component **143**A is directed through air **144**; component **143**B is directed to beam splitter **145**.

In particular, component **143**A of laser radiation **142** directed to air **144** is scattered into scatter field **146**. Scattering of component **143**A is illustrated by scattering vectors **147** in scatter field **146**, whereas return scattering is illustrated by backscattered laser radiation **148**. Component **143**B of the laser radiation **142** is used as a reference for comparison to backscattered laser radiation **148**. Such a comparison is for example useful in determining air parameters such as air speed, since transmitted and received frequencies of the laser radiation may be ascertained for use in a Doppler equation; such a process is explained in greater detail herein below.

In the illustrated embodiment, backscattered laser radiation **148** is received through optics **149**. In one example, optics **149** is a telescope that gathers backscattered laser radiation **148** into a beam **150**. Optics **149** also directs beam **150** to beam splitter **151**, to split beam **150** into two components **150**A/**150**B. Component **150**B of beam **150** passes through vapor filter **152** to detector **153** to produce electronic signal **158** representative of the component **150**B impinging detector **153**; whereas component **150**A is directed by beam splitter **151** to detector **154**.

In one embodiment, detector **154** is a photodetector that receives radiation **150**A and converts it into an electronic signal **155**. Detector **154** connects to a central computer **156** to process electronic signal **155**. Similarly, detector **153** is a photodetector configured for detecting component **150**B, which is filtered by vapor filter **152** as filtered component **157**. Detector **153** converts component **157** to an electronic signal **158** for processing by central computer **156**.

Accordingly, electronic signal **158** corresponds to backscattered laser radiation **148** as filtered by vapor filter **152**; and electronic signal **155** corresponds to unfiltered backscattered laser radiation **150**A. Electronic signal **155** is thus used to nullify certain anomalies as computer **156** processes electronic signal **158**. For example, when processed with electronic signal **158**, signal **155** may be used to remove, from signal **158**, certain laser transmission power fluctuations in filtered component **157** caused by atmospheric changes in air **144**. Such a process is explained in more detail in connection with FIGS. **4**-**7**.

Computer **156** includes lookup tables **170** and **172** that may be utilized to determine temperature and/or pressure as discussed below.

Reference component **143**B of the laser radiation **142** is split into two components **159** and **160** by beam splitter **145**. Component **160** is directed by beam splitter **145** to vapor filter **152** via mirrored surface **161**, to measure filter characteristics, whereas component **159** is directed by beam splitter **145** to detector **162**, to generate electronic signal **163**. Electronic signal **163** is for example used to normalize power fluctuations in the return of backscattered laser radiation **148** caused by power fluctuations in the generation of laser radiation **142** by laser **141**. Such a process is explained in more detail in FIGS. **4**-**7**.

Vapor filter **152** filters component **160** to produce filtered component **164**. Filtered component **164** is directed to detector **165**, via mirrored surface **166**, and then converted to an electronic signal **167**. Central computer **156** processes electronic signal **167** to determine filter characteristics, such as frequencies and suppression features of the band stop region of vapor filter **152**. One such process is also explained in more detail in context of FIGS. **4**-**7**.

It should be noted that while FIG. **2** shows OADS **140** as having free space optical transmission and optical components such as beam splitters **143**, **145** and **151** and mirrors **161** and **166**, optical fiber may be used for laser **141** transmission along paths **142**, **143**A, **143**B, **159**, **160**, **164**, **150**, **150**A, **150**B and/or **157**; in such an embodiment, fiber splitters may be used in place of beam splitters **143**, **151** and **145**, and mirrors **161** and/or **166** may be eliminated.

It will also be appreciated that although the embodiment shown in OADS **140** of FIG. **2** employs vapor filter **152**, other types of filters may be utilized. For example, notch or band-stop filters such as interference filters, dichroic filters, fiber Bragg grating filters and/or Rugate filters may be utilized. A filter used in place of vapor filter **152** may advantageously have properties such as: (1) high optical absorption within a stop-band region on the order of 40-60 dB or more; (2) a notch filter absorption width between about 5 GHz and 40 GHz, with an absorption width under 10 GHz being preferred; and (3) steep absorption sidewalls, with a 10%-90% absorption transition occurring within about 5 GHz or less. Pass-band filters may also be used, such as when they operate in a reflection mode such that a reflection produces a stop-band filter. Single filters with multiple absorption features may be utilized, or optical or fiber splitters may be used to route optical signals through multiple filters, each filter having a single absorption feature.

Filters other than atomic vapor filters may provide certain advantages. For example, while the absorption frequencies of atomic vapor filters are reliably tied to properties of an atomic vapor used, their use may constrain an OADS to include a tunable laser having output at such frequencies. However, certain tunable lasers may have improved performance and/or stability at frequencies that do not conveniently match atomic vapor filter absorption frequencies. Certain filters such as interference filters, dichroic filters, fiber Bragg grating filters and/or Rugate filters may be designed to have absorption features tuned to a preferred frequency output range of a tunable laser, rather than tuning the laser to the filter. The use of a tunable laser selected on its merits, and a matching notch filter in an OADS may thus (1) enable use of higher laser output power for improved return signal strength, (2) make the OADS more robust with respect to thermal stability, vibration and shock, (3) eliminate hazardous materials (e.g., mercury) from the OADS, and/or (4) reduce size, weight and/or cost of the OADS.

FIG. **3** shows one graph **200** useful in illustrating an exemplary air speed calculation with OADS **140**. Graph **200** shows two curves, **201** and **202**, comparing normalized laser radiation magnitudes as a function of frequency (signal strength, that is, normalized laser radiation magnitude, is plotted with respect to axis **205**, and frequency is plotted with respect to axis **204**). Curve **202** exemplifies filtered radiated laser radiation such as that of filtered component **164** of FIG. **2**. As such, curve **202** shows filter characteristics of vapor filter **152** of FIG. **2** determined by processing of electronic signal **167**. Curve **202** shows a peak absorption of filter **152** occurring at a down-translated frequency of 0 GHz. By way of example, the actual peak absorption frequency of filter **152** may be about 1182.5 THz (i.e., having a corresponding wavelength of about 253.7 nm).

Laser radiation **142** generated by laser **141** passes through filter **152** to provide filtered component **164**. Once filtered component **164** is converted to electronic signal **167** by detector **165**, computer **156** analyzes and stores features of vapor filter **152** through digital signal processing of signal **167** (e.g., computer **156** stores reference features, obtained under controlled conditions, for use in future calculations). As shown in this example, features of vapor filter **152** have approximately 10% normalized absorption at approximately +/−5 GHz (i.e., 0.9 normalized transmission factor at approximately +/−5 GHz according to axis **205**) about the peak absorption frequency. Other types of suitable filters may include different absorption/transmission features.

Curve **201** exemplifies filtered backscattered laser radiation such as that of filtered component **157** of FIG. **2**. In one embodiment, curve **201** is used to determine air speed by comparison to curve **202**. For example, curve **202** illustrates how vapor filter **152** affects laser radiation **142**; curve **201** similarly illustrates how vapor filter **152** affects laser radiation **142** as laser radiation **142** is backscattered (e.g., returns as radiation **148**) from air **144**. Frequency shift **203** represents the change in frequency of peak absorption for vapor filter **152** between transmitted laser radiation **142** and returned laser radiation **148**. Computer **156** processes algorithms applying Doppler velocity equation to determine air speed from frequency shift **203**.

To determine air speed in one embodiment, computer **156** determines how far in frequency the peak absorption frequency of filtered component **157** has shifted from the initial laser frequency by comparing curve **202** to curve **201** (e.g., comparing peak absorption frequencies of filtered components **157** and **164**). Frequency shift **203** substantially equates to a radial wind velocity through the Doppler velocity equation:

$$\Delta\nu_D = \frac{2V_R}{\lambda}, \quad \text{(Eq. 1)}$$

where $\Delta\nu_D$ represents the Doppler frequency shift, V_R represents velocity component of the vehicle (e.g., aircraft **101** of FIG. **1**) along the laser direction of propagation **143**A and λ represents the wavelength of laser radiation **142**.

In one embodiment, wind velocity component V_R may be measured by determining the frequency shift from curve **202** of graph **200** as compared to curve **201** of graph **200**. This is accomplished by calculating a symmetry point of each curve **201** and **202** and determining a difference in symmetry points between the two curves.

Vapor filter **152** may have a plurality of absorption features. Consequently, OADS may have a plurality of absorption maxima, such as those illustrated by curves **201** and **202** of FIG. **3**, which may be used to provide a more accurate estimate of the vehicle's velocity. The vehicle's velocity, V_R, may be calculated using equation 1 for each absorption feature. An average velocity of the vehicle may then be calculated from each value of V_R.

FIGS. **4-7** show graphs illustrating exemplary calculations for other air parameters with OADS **140**. For example, after determining frequency shift due to air speed as shown in FIG. **3**, other air parameters such as air temperature and air pressure may be calculated. In one example, computer **156** initially determines an intensity measurement of the detected backscattered laser radiation (e.g., filtered component **157** detected by detector **153**) from electronic signal **158**. This experimentally verified intensity measurement of returned laser radiation corresponds to the following equation:

$$S_S(\nu)=P_L T_L D_S T_R E_S \int d\nu_r \int d\nu_{laser} [L(\nu_{laser}) F(\nu_r-\nu)(rR)(\nu_r-(\nu_{laser}-\Delta\nu_D))+mM(\nu_r-(\nu_{laser}-\Delta\nu_D)))] \quad \text{(Eq. 2)}$$

where $S_S(\nu)$ is electronic signal **158** from detector **153**; P_L is the laser power, T_L is the transmission coefficient through air **144** along laser path **143**A, $L(\nu_{laser})$ is the laser line shape inherent to the laser **141** output as a function of laser frequency ν_{laser}, T_R is the transmission coefficient through air **144** along laser path **148**, E_S is optical efficiency of the detector channel through detector **153**, $F(\nu)$ is the band stop frequency range of vapor filter **152** centered at a frequency of ν, R is Rayleigh scattering as a function of frequency (applicable to the Rayleigh regime) ν_r for backscattered laser radiation minus the quantity of laser frequency ν_{laser} minus the Doppler shift ΔV_D, r is the Rayleigh scattering magnitude coefficient dependent on air density and the Rayleigh backscattering coefficient, M is Mie scattering as a function of ν_r minus the quantity of ν_{laser} minus $\Delta\nu_D$, m is the Mie scattering magnitude coefficient dependent on aerosol concentration and the Mie backscattering coefficient, and D_S is detector **153** efficiency. The Rayleigh backscattering coefficient r and the Mie backscattering coefficient m are constant for a particular atmosphere. These coefficients correspond to the number of scatterers (i.e., molecules for Rayleigh, aerosols for Mie) per unit volume of atmosphere.

Next, computer **156** may determine other air parameters, utilizing the result obtained for the measured intensity of the returned laser energy. Such a process, for example, may begin by determining characteristics of vapor filter **152** by transmitting of reference laser radiation **160** through vapor filter **152**. For example, measuring band stop characteristics of vapor filter **152** with laser **141** (e.g., via component **143**B to electronic signal **167**) during experimentation yields a convolution of the laser wavelength and the filter according to the following equation:

$$S_F(\nu)=P_L E_F D_F \int d\nu_{laser} [L(\nu_{laser}) F(\nu_{laser}-\nu)], \quad \text{(Eq. 3)}$$

where $S_F(\nu)$ is signal **167** from detector **165** as a function of frequency ν (e.g., as illustrated in curve **221** of FIG. **4**); E_F is the optical efficiency of filter **152** collection along paths **160** and **164**, and D_F is detector **165** efficiency.

Note that all optical efficiencies E_F and E_S, capture signal losses that are optical in nature. For example, E_F, the optical efficiency for detector **165**, includes the optical beam splitting ratios for beam splitters **143** and **145**, the optical transmission and coupling across filter **152** and the optical delivery efficiency onto detector **165**. E_S, the optical collection efficiency for detector **153**, includes the collection efficiency of telescope **149**, the optical coupling efficiency into path **150**, the beam splitter ratio of beam splitter **151**, the transmission efficiency across filter **152** and the delivery efficiency onto detector **153**. Detector efficiencies D_F and D_S include the detector conversion efficiencies for detectors **165** and **153**, respectively. Thus, D_F is the conversion efficiency whereby detector **165** converts laser radiation along path **164** into an electrical signal **167**. Likewise, D_S is the conversion efficiency whereby detector **153** converts laser radiation along path **157** into an electrical signal **158**.

Backscattered laser radiation **148** may include power fluctuations that are caused by laser **141** while generating laser radiation **142**. Accordingly, laser radiation detected by detector **162** (e.g., via component **159**) may be utilized to normalize power fluctuations attributable to laser **141**. In one embodiment, detector **162** converts component **159** into electronic signal **163**. In turn, computer **156** processes and normalizes according to the following equation:

$$S_L(\nu)=P_L E_L D_L \int d\nu L(\nu), \quad \text{(Eq. 4)}$$

where $S_L(\nu)$ is the electronic signal **163** from detector **162**, E_L is the optical collection efficiency for detector **162**, D_L is the conversion efficiency of detector **162** and P_L is the power of laser **141**. Note that the optical collection efficiency E_L includes the beam splitting ratios of beam splitters **143** and **145** and the delivery efficiency of laser beam path **159** onto detector **162**.

Curve **221** of graph **220** of FIG. **4** represents the magnitude of laser radiation (component **164**) filtered by vapor filter **152** and normalized between 0 and 1. Curve **221** represents the magnitude of the laser radiation as a function of frequency (i.e., laser radiation magnitude plotted with respect to axis **222** and frequency plotted with respect to on axis **223**). Curve **221**, therefore, illustrates filtered laser radiation via component **160** as determined by computer processing of electronic signal **167**, plotted as laser radiation magnitude normalized between 0 and 1, versus frequency.

In one embodiment, absorption/transmission characteristics of vapor filter **152** are normalized using Eq. 3 and Eq. 4. Eq. 3 yields stop band characteristics of filter **152** and Eq. 4 accounts for power fluctuations in the generation of laser radiation **142**. With the power fluctuations of Eq. 4 substantially removed, a "normalization channel" is created, and power fluctuations attributable to atmospheric changes may be accounted for.

In one embodiment, additional power fluctuations caused by atmospheric changes in air **144** are also removed. For example, laser radiation detected by detector **154** (e.g., via component **150**A) assists in removing laser power fluctuations caused by atmospheric changes in air **144**. Accordingly, detector **154** converts received laser radiation into electronic signal **155**. Computer **156**, in turn, processes electronic signal **155** to determine the normalized laser radiation magnitude according to the following equation:

$$S_N=P_LT_LT_RE_ND_N\int d\nu\int d\nu_{laser}[L(\nu_{laser})(rR(\nu-(\nu_{laser}-\Delta\nu_D))+mM(\nu-(\nu_{laser}-\Delta\nu_D)))] \quad \text{(Eq. 5)}$$

where S_N is the signal **155** from detector **154**; E_N is optical collection efficiency of the detector **154** and D_N is the conversion efficiency of detector **154**.

In one embodiment, it is advantageous to normalize the various characteristic functions to enable a closed-loop solution to the process of determining temperature and pressure. In one example, therefore, computer **156** calculates the normalized laser line shape according to following equation:

$$\int L(\nu_{laser})d\nu_{laser}=1, \quad \text{(Eq. 6)}$$

where (as before) ν_{laser}, is laser line shape frequency and L denotes the laser line shape as a function of frequency. In another example, computer **156** calculates normalized Rayleigh Function according to the following equation:

$$\int R(\nu_r)d\nu_r=1, \quad \text{(Eq. 7)}$$

where R denotes the Rayleigh line shape as a function of frequency ν_r, applicable to the Rayleigh regime. In another example, computer **156** scales the electronic signal **167** recorded from detector **165** by dividing all recorded values by the maximum value according to the following equation:

$$\mathrm{MAX}(S_F(\nu))=1, \quad \text{(Eq. 8)}$$

where MAX denotes an operation that finds a maximum value of a particular function, and S_F denotes electronic signal **167** measured from detector **165**, as a function of frequency ν (e.g. as illustrated in curve **221** of FIG. **4**). In another example, computer **156** normalizes the Mie Function according to the following equation:

$$M(\nu)=\delta(\nu), \quad \text{(Eq. 9)}$$

where δ(ν) is the delta function.

In one embodiment, dividing the signal **167** collected from detector **165** (and represented by Eq. 3, above) by the signal **163** collected from detector **162** (and represented by Eq. 4, above) removes laser **141** power fluctuations, as follows:

$$\frac{S_F(\nu)}{S_L(\nu)}=\frac{P_LE_FD_F\int d\nu_{laser}[L(\nu_{laser})F(\nu_{laser}-\nu)]}{P_LE_LD_L\int d\nu L(\nu)} \quad \text{(Eq. 10)}$$

Equation 10 simplifies to:

$$\frac{S_F(\nu)}{S_L(\nu)}=\frac{E_FD_F}{E_LD_L}LF(\nu) \quad \text{(Eq. 11)}$$

where LF(ν) represents a convolution of functions L and F (that is, a function that represents the effects of functions L and F combined at each frequency ν).

In one embodiment, tuning the laser **141** to a reference frequency ν_{ref} far enough removed from the effects of the vapor filter **152** enables the measurement of the ratio of the optical and detector efficiencies of the signal channels **167** (S_F, represented by Eq. 3 above) and **163** (S_L, represented by Eq. 4 above). This, in turn, enables the normalization of the signal **167** measurement to one, for simultaneously checking for laser, detector and filter abnormalities on a scan-by-scan basis:

$$\frac{S_F(\nu_{ref})}{S_L(\nu_{ref})}=\frac{E_FD_F}{E_LD_L} \quad \text{(Eq. 12)}$$

In one embodiment, LF(ν) are determined to generate a look up table of the convolution of theoretical Rayleigh functions (calculated in terms of temperature and pressure) with the measured filter function. Since the measured filter function is already the convolution of the laser and filter spectra, convolving the Rayleigh function with the measured filter signal **167** yields the expected return signal from an atmosphere of pure Rayleigh scatterers.

In one embodiment, the measured signal **158**, which is the backscatter return from the atmosphere **144** that passes through the vapor filter **152** (and is represented by Eq. 2 above), is divided by the signal **155**, which is the backscatter return from the atmosphere **144** that does not pass through vapor filter **152** (and is represented by Eq. 5 above). This calculation removes changes in signal transmission that are independent of the factors to be measured:

$$\frac{S_S(\nu)}{S_N(\nu)}=\frac{P_LT_LD_ST_RE_S\int d\nu\int d\nu_{laser}\left[\begin{matrix}(L(\nu_{laser})F(\nu_r-\nu))\\ \begin{pmatrix}rR(\nu_r-(\nu_{laser}-\Delta\nu_D))+\\ mM(\nu_r-(\nu_{laser}-\Delta\nu_D))\end{pmatrix}\end{matrix}\right]}{P_LT_LT_RE_ND_N\int d\nu\int d\nu_{laser}\left[\begin{matrix}L(\nu_{laser})\\ \begin{pmatrix}rR(\nu_r-(\nu_{laser}-\Delta\nu_D))+\\ mM(\nu_r-(\nu_{laser}-\Delta\nu_D))\end{pmatrix}\end{matrix}\right]} \quad \text{(Eq. 13)}$$

Since M is a delta function, Equation 13 simplifies to:

$$\frac{S_S(\nu)}{S_N(\nu)}=\left[\frac{E_SD_S}{E_ND_N}\right]\frac{rLFR(\nu_{laser}-\Delta\nu_D)+mLF(\nu_{laser}-\Delta\nu_D)}{r+m} \quad \text{(Eq. 14)}$$

where LFR(ν) represents a convolution of functions L, F and R in the sense of the convolution LF(ν) discussed above.

In one embodiment, tuning laser **141** to reference frequency ν_{ref} far enough removed from the effects of the vapor filter **152** enables the measurement of the ratio of the optical and detector efficiencies of the signal channels **158** (S_S as represented by Eq. 2 above) and **155** (S_N as represented by Eq. 5 above). This enables a check for abnormalities in the filter on a scan-by-scan basis:

$$\frac{S_S(\nu_{ref})}{S_N(\nu_{ref})} = \frac{E_S D_S}{E_N D_N} \quad \text{(Eq. 15)}$$

In one embodiment, a variable K_{ref} may be defined as:

$$K_{ref} = \frac{S_S(\nu_{ref})}{S_N(\nu_{ref})} \quad \text{(Eq. 16)}$$

Once both data sets (i.e., S_S and S_N) are symmetric about the same data point, computer **156** calculates temperature and pressure from the return signal. Initially, computer **156** uses theoretical Rayleigh functions that are functions of temperature and pressure in conjunction with the measured filter transmission to generate a lookup table **170** that stores laser, Rayleigh, and filter (LFR(ν)) convolutions that are dependent on atmospheric temperature and pressure. Computer **156** may then compare a normalized return signal to a value stored in lookup table **170** to determine atmospheric temperature and pressure. In order to compare the return signal with the lookup table **170**, computer **156** accounts for the magnitude of Mie scatterers as well as any changes in air density that may change the magnitude of the Rayleigh signal.

A vapor filter may be used as a bandstop filter; such filters typically provide frequency stability, optical depth, and optimal filter shape. For the purposes of separating the Rayleigh and Mie scattering, an optical depth of approximately 60 dB provides excellent absorption of Mie scattering within a small frequency variance around ν_0 (i.e., where ν_f is a normalized frequency of 0 GHz). For example, an atomic vapor filter may provide 60 dB of absorption in a frequency region that is not contaminated by Mie scattering. This region may be used in acquiring initial estimates of pressure and temperature (explained below in FIG. **5**). Such absorption is observable in FIG. **5** below as the measured signal S_F which has the magnitude of zero centered about ν_0. This data provides information about pure Rayleigh scattering that may be used to calculate the ratio of Mie scattering to Rayleigh scattering, as shown in Eq. 17:

$$\frac{S_S(\nu_0)}{S_N(\nu_0)} = \left[\frac{E_S D_S}{E_N D_N}\right]\frac{rLFR(\nu_0) + mLF(\nu_0)}{r+m} \quad \text{(Eq. 17)}$$

Since the vapor filter fully attenuates the Mie scattering in this region:

$$\frac{S_S(\nu_0)}{S_N(\nu_0)} = \left[\frac{E_S D_S}{E_N D_N}\right]\frac{rLFR(\nu_0)}{r+m}, \quad \text{(Eq. 18)}$$

where $LFR(\nu_0)$ is the value of the theoretical return signal at particular atmospheric temperature and pressure. Accordingly, computer **156** calculates the ratio of Mie scattering by first defining a variable K_0 as follows:

$$K_0 = \frac{S_S(\nu_0)}{S_N(\nu_0)} \quad \text{(Eq. 19)}$$

and then solving for the ratio

$$\frac{m}{r} = \frac{K_0}{K_a}LFR(\nu_0) - 1 \quad \text{(Eq. 20)}$$

Using the normalized signal return in the region of interest (i.e., the sloped region between the minimum and maximum of the signal return) and writing the result in terms of the ratio of m over r, yields the following:

$$\frac{S_S(\nu)}{S_N(\nu)} = K_a \frac{LFR(\nu) + \frac{m}{r}LF(\nu)}{1 + \frac{m}{r}} \quad \text{(Eq. 21)}$$

Substituting the ratio of m and r of Eq. 20 into Eq. 21 yields:

$$\frac{S_S(\nu)}{S_N(\nu)} = K_a \frac{LFR(\nu)}{LFR(\nu_0)} + LF(\nu)\left[1 - \frac{K_0}{K_a LFR(\nu_0)}\right] \quad \text{(Eq. 22)}$$

Solving for LFR(ν) yields:

$$LFR(\nu) = \frac{S_S(\nu)}{S_N(\nu)}\frac{LFR(\nu_0)}{K_a} + LF(\nu)\left[\frac{1}{K_a} - \frac{LFR(\nu_0)}{K_0}\right], \quad \text{(Eq. 23)}$$

where the measured signal return LFR(ν) is written in terms of measured quantities and the theoretical values of $LFR(\nu_0)$. Computer **156** then calculates LFR(ν) and compares it to the lookup table **170** to determine atmospheric temperature and pressure, described in greater detail in FIG. **5**.

Accounting for power fluctuations, optical efficiencies and detector efficiencies as described herein allows for an independent check on vapor filter **152** while OADS **140** operates. With variable characteristics of detector channels and power fluctuations accounted for, computer **156** may determine, for example, the substantially constant characteristics of vapor filter **152**, such that more accurate measurements of received backscattered laser radiation (e.g., laser radiation **148**) are obtained.

In one embodiment, the normalization channel depicted in FIG. **4** is used to remove atmospheric power fluctuations of laser radiation **148**. In doing so, computer **156** measures Rayleigh and Mie components of laser radiation **147** in terms of optical efficiencies and detector efficiencies. Such efficiencies are typically measured on a shot-by-shot basis during the analysis process. In an exemplary embodiment of operation, laser **141** generates and transmits laser radiation **142** as a series of pulses at a particular pulse repetition frequency ("PRF"), while in other embodiments laser **141** is a continuous wave laser (as discussed in connection with FIG. **2**). Computer **156** then measures the Rayleigh and Mie components in terms of optical efficiencies and detector efficiencies on a pulse-by-pulse basis.

To measure Rayleigh components and Mie components, in one embodiment, OADS **140** tunes the frequency of the laser radiation **142** transmitted by laser **141**. For example, laser **141** transmits the laser radiation **142** at distal frequencies from the peak absorption frequency of filter **152** (illustrated by ν_f in FIG. **4**) to provide a frequency-independent measurement. Computer **156** then determines the line shape of laser radiation **142** through filter **152**.

In one embodiment, measured intensity of the detected backscattered laser radiation (e.g., as determined by electronic signal **158**) is functionally compared to normalized atmospheric factors. The measured intensity often depends upon Mie scatterers (e.g., aerosols) and air density changes due to altitude changes and temperature changes. The air density changes and the temperature changes are not, however, removed through the normalization processes described herein. For computer **156** to accurately determine air parameters such as temperature and pressure of air **144**, air density changes are removed from the detected backscattered laser radiation so that computer **156** may accurately determine the air parameters.

FIG. **5** shows graph **240** with curves **241** (detected backscattered laser radiation at a higher air density causing both Rayleigh and Mie scattering), **242** (detected backscattered laser radiation at an air density causing Rayleigh scattering) and **243** (normalized Rayleigh scattering). Curves **241**, **242** and **243** illustrate laser radiation magnitudes (plotted with respect to axis **250**) as a function of frequency (plotted with respect to axis **251**). In one embodiment, computer **156** processes data from curves **241**, **242** and **243** to determine other air parameters. For example, Mie scattering effects are substantially isolated and removed from calculations to determine air temperature and air pressure, since these Mie scattering effects produce inaccurate measurements due to inconsistent aerosol concentrations.

In one embodiment, to determine the air temperature and air pressure, computer **156** processes the data from curves **241**, **242** and **243** to substantially isolate and remove the Mie scattering effects, such as those found in curve **241**. In processing the data from curves **241**, **242** and **243**, computer **156** calculates lookup table **170** in substantially real time using a measured laser/filter profile (i.e., as measured at detector **165** of FIG. **2**) convolved with theoretical Rayleigh functions for a particular temperature and pressure (e.g., illustrated by curves **242** and **243**). Computer **156** then scales the measured return signal LFR(ν) (i.e., illustrated by curve **241** in this example) with the ratio of m to r determined by Eq. 20. Computer **156** then analyzes data near the deepest portion of the filter attenuation (i.e., approximately +/−0.5 GHz from ν_f) to estimate pressure and/or temperature. This portion corresponds to a 60 dB region of absorption that is not contaminated by Mie scattering. Use of this region is a preferred aspect of the calculation technique that provides temperature and pressure accuracy by providing a reliable temperature base from which to increment temperature and/or pressure estimates.

Computer **156** calculates theoretical Rayleigh return assuming an initial temperature estimate and performs a Least Square Error (LSE) calculation to determine the accuracy of the temperature with respect to the theoretical Rayleigh function. Computer **156** repeats the process with incremental changes to temperature and/or pressure until an optimal fit (i.e., an LSE calculation that corresponds to design specifications) is achieved. Although discussed in detail with respect to LSE, other approximation methods, such as Newton-Raphson and Monte Carlo, may be used in alternative embodiments. Accordingly this disclosure teaches by way of example and not by limitation.

Temperature affects air density in a manner that is reciprocal to pressure; increasing pressure increases density, while increasing temperature decreases density. Additionally, increasing temperature increases the Rayleigh lineshape width while increasing pressure increases the Rayleigh lineshape height. Accordingly, for each incremental value of temperature and/or pressure, the Rayleigh lineshape is unique. Such scattering theory is discussed in "On The Kinetic Model Description Of Rayleigh-Brillouin Scattering From Molecular Gases", G. C. Tenti, D. Boley and R. C. Desai, Canadian Journal of Physics, vol. 52, pg. 285-290 (1974).

In one example, computer **156** determines air density changes by aligning peak absorption frequencies of curves **241**, **242** and **243**, illustrated at frequency ν_f. Since curve **243** represents detected backscattered laser radiation containing substantially no Mie scattering, curve **243** may be used as a reference where Mie scattering has been eliminated. In one example, computer **156**, therefore, uses curve **243** to remove the effects of Mie scattering by aligning curves **241**, **242** and **243** and by calculating a ratio of the detected backscattered laser radiation to theoretically pure Rayleigh scattering (the ratio of curves **241** and **242**) which may be utilized to determine air density. Mie scattering effects are then removed by subtracting curve **243** from the calculated ratio of curves **241** and **242**. With Mie scattering essentially removed from the measurement, computer **156** more accurately determines air temperatures and air pressures.

FIGS. **6** and **7** show other exemplary graphs that may be used in determining air pressure and air temperature. FIG. **6** illustrates a graph **260** of electronic signals **163** and **167** of FIG. **2** respectively generated by detectors **162** and **165** of FIG. **2**. Graph **260** shows electronic signals **163** and **167**, that represent light intensity as a function of normalized signal strength (axis **261**), versus frequency (axis **262**). FIG. **7** illustrates a graph **280** of electronic signals **158** and **155** (see FIG. **2**) generated by detectors **153** and **154** respectively, representing light intensity as a function of normalized signal strength (axis **281**), versus frequency (axis **282**). These four light intensities (represented by electronic signals **163**, **167**, **158** and **155**) may be measured, over time, through transmission and collection of light corresponding to laser pulses, or they may be measured through transmission and collection of light corresponding to a continuous wave laser whose frequency varies continuously. In one example, a transmission frequency of laser radiation **142** of FIG. **2** generated by laser **141** at a certain PRF may sweep such that each laser pulse is emitted at a different frequency. Electronic signals **163** and **167** therefore illustrate how laser radiation **142** of laser **141** may sweep in frequency across an absorption band **263** of the vapor filter **152**. Illustratively, FIG. **6** shows one complete frequency sweep of laser radiation **142** generated by laser **141** and detected by detectors **162** and **165**. Similarly, electronic signals **155** and **158** of FIG. **7** show detected signals of detectors **153** and **154** as laser radiation **142** of laser **141** performs a complete sweep in frequency across absorption band **283** of vapor filter **152**.

From signals **163** and **167**, computer **156** may for example determine a normalized filter transmission, by dividing discrete points of electronic signal **167** by corresponding discrete points of signal **163**. Similarly, computer **156** may determine a normalized atmospheric return though vapor filter **152** by dividing discrete points of signal **158** by corresponding discrete points of signal **155**. These discrete points, described herein, correspond to individual pulses of laser radiation **142**.

Using normalized calculations of filter transmission (e.g., from graph **260**) and the normalized calculations of atmospheric return (e.g., from graph **280**), computer **156** determines relative optical efficiencies in the vapor filter **152**.

In one embodiment, computer **156** determines optical transmission for vapor filter **152** using the frequency independent components of data from graph **260**, FIG. **6** (there is substantially no change in amplitude for signals **163** and **167** at frequencies greater in magnitude than ±18 GHz from 0 GHz illustrated at points **264**, **265**, **266** and **267**). Computer **156** therefore determines a ratio of optical transmission for vapor filter **152** by calculating a ratio of signal **167** to signal **163**, via frequency corresponding points of the signals, for points representing frequencies greater in magnitude than ±18 GHz from 0 GHz.

Similarly, computer **156** determines a magnitude of intensity of atmospheric-returned laser radiation received through vapor filter **152** using the frequency independent parts of the data from graph **280**, FIG. **7** (there is substantially no change in amplitude for signals **155** and **158** at frequencies greater in magnitude than ±18 GHz from 0 GHz illustrated at points **284**, **285**, **286** and **287**). Computer **156** thereby determines a ratio of atmospheric return with the laser power measurement by calculating a ratio of signal **158** to signal **155** via frequency corresponding points of the signals for points representing the frequencies greater in magnitude than ±18 GHz from 0 GHz.

In one embodiment, computer **156** calculates a ratio of signal **158** to signal **155** for frequencies between ±0.5 GHz (illustrated at points **288** and **289**). Such a frequency range includes substantially no Mie scattering of laser radiation **142** for air **144**; it thus corresponds to substantially pure Rayleigh scattering. Computer **156** thus compares a Rayleigh to Mie scattering strength based upon the ratio of signal **158** to signal **155**. Computer **156** determines Rayleigh to Mie scattering strength by comparing a ratio of signal **158** to signal **155** at frequencies between ±0.5 GHz to the ratio of signal **158** to signal **155** at frequencies greater than ±18 GHz from 0 GHz. In one embodiment, computer **156** performs similar calculations for "non-scattered" laser radiation **142** (e.g., component **143**B of FIG. **2**) based on data illustrated in FIG. **6** using points **268** and **269**. Such a process is further described in FIG. **8**.

Ratios determined for the non-scattered laser radiation **142** and for the scattered laser radiation **142** may be used in tandem to numerically calculate Laser-Rayleigh-Filter convolution (e.g., LRF(v)) from data. The Laser-Rayleigh-Filter convolution is in turn compared to a look up table of theoretical Laser-Rayleigh-Filter convolution values to determine temperature and pressure.

FIG. **8** shows a flowchart of one exemplary methodical operation **400** of an OADS. Method **400** may be partially or fully performed by computer **156** of OADS **140**; computer **156** may receive operating instructions from software and/or firmware. A laser (e.g., laser **141** of FIG. **2**) sweeps laser radiation across a predetermined frequency spectrum, in step **401**. The laser may sweep the laser radiation across a frequency range of about +/−20 GHz by transmitting laser radiation at a certain PRF (or it may sweep frequency continuously, as discussed in connection with FIG. **2** above). In one embodiment, the PRF is about 1 kHz, with a pulse width between about 50 ns and 100 ns, and a swept frequency range is centered about a frequency corresponding to a peak absorption frequency (e.g., 260 nm) of a filter (e.g., vapor filter **152**, FIG. **2**).

Laser radiation is typically split into four distinct paths such that the laser radiation may be detected as four different inputs, in step **402**. These four paths of laser radiation correspond to: 1) laser radiation transmitted by the laser (e.g., component **159** of FIG. **2**); 2) laser radiation transmitted by the laser through the filter (e.g., component **164** of FIG. **2**); 3) laser radiation transmitted by the laser into the air and backscattered (e.g., component **150**A of FIG. **2**); and 4) laser radiation transmitted by the laser into the air and backscattered through the filter (e.g., component **157** of FIG. **2**). For simplicity, these components are hereinafter referred to as: 1) unfiltered laser radiation; 2) filtered laser radiation; 3) unfiltered backscattered laser radiation or unfiltered scattered laser radiation; and 4) filtered backscattered laser radiation or filtered scattered laser radiation.

After detecting the four components of laser radiation, a computer (e.g., computer **156**, FIG. **2**), determines normalized filter transmission of the vapor filter, in step **403**. For example, the computer, in one embodiment, processes the unfiltered laser radiation and filtered laser radiation by dividing the magnitude of the filtered laser radiation by the magnitude of the unfiltered laser radiation. In one embodiment, the division is performed on a pulse by pulse basis, where divided magnitudes of the pulses have corresponding frequencies.

The computer also determines, in one embodiment, a normalized atmospheric return of the laser radiation, in step **404**. For example, the computer may process the filtered backscattered laser radiation and unfiltered backscattered laser radiation by dividing the magnitude of the filtered backscattered laser radiation by the magnitude of the unfiltered backscattered laser radiation. Again, in one embodiment, division is performed on a pulse by pulse basis, where divided magnitudes of the pulses have corresponding frequencies.

Once normalized filter transmission and normalized atmospheric return of the laser radiation are determined, the computer determines signal strengths for each of the filter transmission and the atmospheric return. For example, the computer determines the optical transmission through the filter by calculating a ratio of the filtered laser radiation to the unfiltered laser radiation at particular frequency ranges, in steps **405** and **407**. The computer similarly determines the atmospheric return (scattering) signal strength through the filter by calculating a ratio of the filtered backscattered laser radiation to the unfiltered laser radiation at particular frequency ranges, in steps **406** and **408**.

The computer also determines a signal strength ratio for the normalized filter transmission by dividing filtered laser radiation by unfiltered laser radiation, again on a pulse by pulse basis, at frequencies greater in magnitude than about +/−18 GHz about the peak absorption frequency, in step **407**. The computer further determines a signal strength ratio for the normalized filter transmission by dividing filtered laser radiation by unfiltered laser radiation on a pulse by pulse basis at frequencies between about +/−0.5 GHz, in step **405**. These signal strength determinations correspond to frequency ranges where Mie scattering (e.g., +/−18 GHz) and Rayleigh scattering (e.g., +/−0.5 GHz) are most prevalent, and are thus useful when combined with similar signal strength determinations for the normalized atmospheric return. The computer determines a Mie scattering signal strength ratio for the normalized atmospheric return of the laser radiation by dividing filtered backscattered laser radiation by unfiltered backscattered laser radiation, again on a pulse by pulse basis, at frequencies greater in magnitude than about +/−18 GHz about the peak absorption frequency, in step **408**. The computer also determines a Rayleigh scattering signal strength ratio for the normalized atmospheric return of the laser radiation by dividing filtered scattered laser radiation by unfiltered backscattered laser radiation on a pulse by pulse basis at frequencies between about +/−0.5 GHz in step **406**.

With signal optical transmission for the filter and signal strengths for both Rayleigh scattering and Mie scattering determined, the computer determines a Rayleigh laser filter convolution in step **409**. For example, the computer, in one embodiment, performs a convolution of the optical transmission with the Rayleigh and Mie scattering signal strengths corresponding to the frequency ranges for Rayleigh and Mie scattering of +/−0.5 GHz and +/−18 GHz, respectively. The computer then accesses a lookup table, such as lookup table **170** of FIG. **2**, that has theoretical Rayleigh laser filter convolution values to determine temperature and pressure of the air, in step **410**.

It is also possible to calculate a convolution of a measured filter function with a theoretical Rayleigh-Brillouin return (Rayleigh line shape), and directly compare the convolution with filtered scattered laser radiation. This allows calculation of atmospheric parameters without calculating a deconvolution of the Rayleigh-Brillouin signal, reducing the complexity of real-time calculations required to determine the atmospheric parameters. In particular, ratios of measured signals may be compared directly to theoretical ratios of a Rayleigh line shape convolved with measured filter functions to allow self calibrating measurements. For example, signal strength variations across data gathering channels and power of scattered laser radiation may be inherently normalized when such ratios are used. Certain ratios of measured data at laser frequencies that lie within filtered bands of band-stop filters (e.g., absorption features of an atomic vapor cell, or equivalent features of other filters, as discussed above) may be useful for determining temperature and pressure, since Mie scattering is eliminated from the measured data. Calculation of convolutions may represent a lower computational burden on a computer (e.g., computer **156** of OADS **140**) as compared to calculating deconvolutions of measured data into and out of a Rayleigh-Brillouin representation.

For example, filtered scattered laser radiation data in a signal channel may characterized by the equation:

$$S_S(\nu)=P_L T_L T_R E_S D_S \iint d\nu_1 d\nu_r L(\nu_{laser}) F(\nu_1-\nu)(rR(\nu-(\nu_r-\Delta\nu_D))+mM(\nu-(\nu_r-\Delta\nu_D))) \quad \text{(Eq. 24)}$$

where parameters are as previously defined, and a subscript **1** indicates a measurement frequency 1. Eq. 24 may be simplified by using the notation LFR(ν) for the convolution of laser, filter function and Rayleigh return, as defined above, and a similar notation LFM(ν) for a convolution of laser, filter function, and Mie scattering return:

$$S_S(\nu_1)=P_{L1}T_{L1}T_{R1}E_{S1}D_{S1}[rLFR(\nu_1)+mLFM(\nu_1)] \quad \text{(Eq. 25)}$$

If frequency 1 is located in a filter absorption band, the Mie scattering term is effectively eliminated, yielding:

$$S_S(\nu_1)=P_{L1}T_{L1}T_{R1}E_{S1}D_{S1}rLFR(\nu_1) \quad \text{(Eq. 26)}$$

Forming a ratio of a signal obtained at frequency 1 with a signal obtained at another frequency 2 in another filter absorption band yields:

$$\frac{S_S(\nu_1)}{S_S(\nu_2)}=\left[\frac{P_{La}L_{La}T_{Ra}E_{Sa}D_{Sa}}{P_{Lb}L_{Lb}T_{Rb}E_{Sb}D_{Sb}}\right]\left[\frac{r_a(r_b+m_b)}{r_b(r_a+m_a)}\right]\left[\frac{LFR(\nu_1)}{LFR(\nu_2)}\right] \quad \text{(Eq. 27)}$$

where frequency 1 is measured at time a and frequency 2 is measured at time b. If times a and b are close enough to each other that no atmospheric changes occur between time a and time b (or if measurements are interspersed in such a way that average values of parameters such as P, L, T, E, D and r are identical over a time span of the measurements) then the ratio of Eq. 27 simplifies further to:

$$\frac{S_S(\nu_1)}{S_S(\nu_2)}=\frac{LFR(\nu_1)}{LFR(\nu_2)} \quad \text{(Eq. 28)}$$

In one embodiment, a lookup table stores temperature and pressure pairs that correspond with two of the measurement ratios defined in Eq. 28. The two ratios essentially define two equations with two unknowns (i.e., a single such ratio may not determine both pressure and temperature). Data may also be taken in more than three filtered bands, yielding more than two of the Eq. 28 ratios; when more than two such ratios are available, multiple values of temperature and pressure may be determined that may be averaged or used in "best fit" methods to improve temperature and pressure determination in a noisy measurement environment.

In an embodiment, theoretical Rayleigh line shapes corresponding to temperature and pressure combinations are stored in a lookup table. A reference curve is calculated by obtaining a Rayleigh line shape corresponding to an estimated temperature and pressure from the lookup table and convolving the Rayleigh line shape with a normalized atmospheric return curve. Values of LFR(ν) at absorption feature maxima may then be determined from the reference curve and used to determine one or more air parameters (e.g. temperature and/or pressure) using Eq. 28.

Calculating convolution of the measured filter function with the theoretical Rayleigh line shape also enables utilization of curve fitting routines to map the convolved curves to true temperature and pressure conditions, such that the deconvolution calculations suggested by the Tenti, Boley and Desai paper above are not required. An OADS may store a precompiled table of stored curve shapes that are generated by modeling large databases of known temperature and pressure values (e.g., the table may be stored in computer **156** of OADS **140**). As measurements are taken, data curves may be generated from measured data, and curve-fitting routines may be used to compare the data curves to the stored curve shapes to derive true temperature and pressure. The utilization of curve-fitting routines may also have less sensitivity to noisy data, as compared to deconvolution calculations, making the determination of true temperature and pressure more robust.

FIG. **9** is a flowchart showing one exemplary method of operation **450** of an OADS, which may be used to calculate one or more air parameters. Method **450** may be partially or fully performed by computer **156** of OADS **140**; computer **156** may receive operating instructions from software and/or firmware.

In an embodiment of step **460**, a laser (e.g., laser **141** of FIG. **2**) sweeps laser radiation across a predetermined frequency range (swept frequency range) that is centered about a deep absorption line of a filter. The laser may sweep the laser radiation across a swept frequency range of about +/−20 GHz by transmitting the laser radiation at a certain PRF, or by sweeping the frequency of a continuous wave laser. In one embodiment, a PRF is about 1 kHz, with a pulse width between about 50 ns and 100 ns, and the swept frequency range is centered about a frequency corresponding to a peak absorption frequency (e.g., 260 nm) of a filter (e.g., vapor filter **152**, FIG. **2**, or an interference filter, a fiber Bragg grating filter, a dichroic filter or a Rugate filter). In an embodiment, the swept frequency range includes frequencies corresponding to at least two absorption features of at least one band stop filter. In another embodiment, the swept frequency range includes frequencies corresponding to at least three absorption features of at least one band stop filter.

Step **462** detects laser radiation corresponding to filtered scattered laser radiation (e.g. component **157** of FIG. **2**), filtered laser radiation (e.g. component **164** of FIG. **2**), and unfiltered laser radiation (e.g. component **159** of FIG. **2**) at each frequency; each step **460** and **462** is for example performed for each laser pulse in the swept frequency range.

Step **464** determines a normalized filter transmission curve by dividing a magnitude of filtered laser radiation by a magnitude of unfiltered laser radiation for each pulse in the swept frequency range; step **466** determines a normalized atmospheric return curve by dividing a magnitude of filtered scattered laser radiation by a magnitude of unfiltered laser radiation for each pulse in the swept frequency range. It will be appreciated that since the data required for the calculations in steps **464** and **466** are collected by the operation of steps **460** and **462**, steps **464** and **466** may be done in any order or in parallel.

Step **468** calculates a Doppler shift $\Delta\nu_D$ that is a frequency shift between the normalized filter transmission curve (calculated in step **464**) and the normalized atmospheric return curve (calculated in step **466**), then calculates a local radial wind velocity ν_R using Eq. 1 above. As was stated above, a band stop filter may have a plurality of absorption features; consequently, a plurality of Doppler shift $\Delta\nu_D$ and radial wind velocity ν_R calculations may be calculated in step **468**.

Step **470** utilizes only normalized atmospheric return curve magnitude values (calculated in step **466**) within three or more specific filter absorption bands to form two or more normalized atmospheric return ratios (actual ratios). For example, if atmospheric return data is derived for frequencies 1, 2, and 3 (at times that are close enough together, as discussed with reference to Eq. 28 above), then two ratios may be formed using one of the frequencies as a baseline (denominator), such as

$$\frac{S_S(\nu_1)}{S_S(\nu_2)} \text{ and } \frac{S_S(\nu_3)}{S_S(\nu_2)}.$$

Atmospheric return curve magnitude values corresponding to absorption feature maxima of one or more band stop filters may be used. One atmospheric return ratio (actual ratio) may be determined if for example only one air parameter (e.g. pressure or temperature) is to be calculated.

Step **472** obtains theoretical temperature and pressure data from a lookup table of normalized filter transmission convolved with theoretically derived Rayleigh line shapes, at the frequencies utilized in step **470**. One or more air parameters (e.g. temperature and/or pressure) are then estimated. A Rayleigh line shape corresponding to the estimated one or more air parameters is for example obtained from a lookup table. A reference curve is then calculated by convolving the Rayleigh line shape with the normalized filter transmission curve from step **464**.

In step **474**, ratios corresponding to the ratios formed in step **470** are formed from magnitude values of the reference curve calculated in step **472**. The ratios formed in step **474** may be referred to as reference ratios.

In step **476**, one or more air parameters (e.g. temperature and pressure) are determined. An error corresponding to the differences between the one or more actual ratios and the corresponding one or more reference ratios may be calculated: if the error is within an acceptable range, the estimated one or more air parameters (corresponding to the Rayleigh line shape) are published as the actual one or more air parameters; but if the error is not within an acceptable range, steps **472**, **474**, and **476** are repeated with one or more different estimated air parameters until the error is within an acceptable range.

The error of step **476** may be calculated using a least mean square error algorithm. Steps **470**, **474**, and **476** may be optional; the normalized atmospheric return curve calculated in step **466** is for example correlated to the reference curve calculated in step **472** using curve fitting routines.

Certain advantages of embodiments described above may include:

(1) Obtaining accurate computations of various air parameters, such as air speed, air temperature and air pressure, substantially regardless of altitude and/or Mie scattering;

(2) Obtaining a system that accurately performs in a variety of vibrational environments;

(3) Obtaining an ability to determine temperature and pressure within a particular region of atmosphere without a prior knowledge of the atmosphere;

(4) Reducing need for on-aircraft system calibrations and system health checks, as compared to existing systems;

(5) Providing robustness with respect to high vibration environments;

(6) Obtaining faster calculations and/or reduced computational requirements placed on aircraft computers, as compared to existing systems;

(7) Ability to accurately calculate velocity in environments with changing temperature and/or pressure; and/or

(8) Ability to accurately calculate one or more air parameters (e.g. velocity, temperature, and/or pressure) without precise control of laser frequency.

Since certain changes may be made in the above methods and systems without departing from the scope of the disclosure herein, it is intended that all matter contained in the above description or shown in the accompanying drawings be interpreted as illustrative and not in a limiting sense. By way of example, those skilled in the art should appreciate that the OADS and the OADS transceivers, as described herein, may be constructed, connected, arranged, and/or combined in ways that are equivalent to what is shown.

What is claimed is:

1. A method for remotely sensing air outside a moving aircraft, comprising generating laser radiation within a swept frequency range;

projecting a portion of the laser radiation from the aircraft into the air to induce scattered radiation;

detecting filtered scattered laser radiation, filtered laser radiation, unfiltered scattered laser radiation, and unfiltered laser radiation;

determining a normalized filter transmission and a normalized atmospheric return from the filtered scattered laser radiation, filtered laser radiation, unfiltered scattered laser radiation, and unfiltered laser radiation; and

determining a plurality Doppler line shifts and a plurality of radial wind velocities from a plurality of frequency shifts between the normalized filter transmission and the normalized atmospheric return, each frequency shift corresponding to an absorption feature of at least one band stop filter.

2. The method of claim **1**, wherein the at least one band stop filter is selected from the group consisting of a fixed frequency atomic vapor filter, an interference filter, a dichroic filter, a fiber Bragg grating filter, a Rugate filter, and combinations thereof.

3. The method of claim **1**, the step of generating comprising generating the laser radiation in pulses, each pulse having a different peak frequency within the swept frequency range.

4. The method of claim 1, the step of generating comprising sweeping a frequency of a laser continuously across the swept frequency range.

5. The method of claim 1, wherein the swept frequency range includes frequencies corresponding to at least two absorption features of the at least one band stop filter.

6. A software product comprising instructions, stored on computer-readable media, wherein the instructions, when executed by a computer, perforin the steps for remotely sensing air outside a moving aircraft, comprising:

instructions for generating laser radiation within a swept frequency range;

instructions for determining a normalized filter transmission and a normalized atmospheric return from filtered scattered laser radiation, filtered laser radiation, unfiltered scattered laser radiation, and unfiltered laser radiation; and

instructions for determining a plurality Doppler line shifts and a plurality of radial wind velocities from a plurality of frequency shifts between the normalized filter transmission and the normalized atmospheric return, each frequency shift corresponding to an absorption feature of at least one band stop filter.

* * * * *